

Time crystallinity in open quantum systems

Andreu Riera-Campeny¹, Mariona Moreno-Cardoner¹, and Anna Sanpera^{1,2}

¹Física Teòrica: Informació i Fenòmens Quàntics. Departament de Física, Universitat Autònoma de Barcelona, 08193 Bellaterra, Spain

²ICREA, Passeig Lluís Companys 23, 08001 Barcelona, Spain.

July 2, 2022

Time crystals are genuinely non-equilibrium quantum phases of matter that break time-translational symmetry. While in non-equilibrium closed systems time crystals have been experimentally realized, it remains an open question whether or not such a phase survives when systems are coupled to an environment. Although dissipation caused by the coupling to a bath may stabilize time crystals in some regimes, the introduction of incoherent noise may also destroy the time crystalline order. Therefore, the mechanisms that stabilize a time crystal in open and closed systems are not necessarily the same. Here, we propose a way to identify an open system time crystal based on a single object: the Floquet propagator. Armed with such a description we show time-crystalline behavior in an explicitly short-range interacting open system and demonstrate the crucial role of the nature of the decay processes.

1 Introduction and outline

Statistical mechanics has been extremely successful in describing the behavior of systems at equilibrium and, occasionally, even the relaxation towards it. During the last decades, countless efforts have been devoted to genuinely non-equilibrium systems. In particular, a lot of attention has been drawn to non-equilibrium *Floquet* systems, i.e., systems undergoing time-periodic dynamics. Those systems have found numerous applications that go from thermal machines and transport [1–5], to *Floquet engineering* [6–8], as well as the discovery of non-equilibrium phases of matter [9–18]. This work focuses on the latter, the so-called time crystals.

A system has *discrete time-translational symmetry* if the generator of the evolution, at any time t , is invariant under the transformation $t \mapsto t + T$, where T is the period. The pioneering ideas of time-crystals proposed in [19] and polished by subsequent discussions in [20], led to the concept of *discrete time crystals* (DTCs), first put forward in [11, 15] and then experimentally realized in [13, 14]. A discrete time crystal is a system that breaks discrete time-translational symmetry showing robust subharmonic response (to be precised below). Closed quantum systems might display oscillations in a wide variety of scenarios; e.g., from Rabi oscillations of quantum optical systems to Bloch oscillations in lattices. Hence, criteria on how to identify a time crystal are essential to understand this non-equilibrium phase of nature. In *closed* systems, a discrete time crystal phase is characterized by an observable \mathbf{O} acting as an *order parameter* whose expectation value $f(t) = \text{tr}[\mathbf{O}\rho(t)]$ must fulfill the three following conditions: [10, 21, 22]:

Andreu Riera-Campeny: andreu.riera.campeny@uab.cat

- (I) **Time-translation symmetry breaking:** the order parameter is less symmetric than the Hamiltonian, i.e., $f(t+T) \neq f(t)$ when $\mathbf{H}(t+T) = \mathbf{H}(t)$. For the DTC we recover $f(t)$ after an integer number of periods $N > 1$, $f(t+NT) = f(t)$.
- (II) **Rigidity of the oscillations:** $f(t)$ shows a fixed oscillation period NT without fine-tuned Hamiltonian parameters. Equivalently, the oscillations should *lock-off* at frequency $2\pi/(NT)$.
- (III) **Persistence to infinite time:** the non-trivial oscillation with period T must persist for infinitely long time in the thermodynamic limit.

Nevertheless, it is not clear whether this phase of matter survives the action of an environment or, even more interesting, if the environment can help to stabilize it [12]. For instance, the discrete time crystal appearing in a disordered one dimensional Ising spin chain (the so-called π SG) cannot survive the coupling to an environment [23]. As a result, efforts have been redirected towards the study of open *mean-field* models with long-range interactions [17, 18, 24] or short-ranged perturbations from them [25] coupled to an environment. In such models, some signatures of time crystallinity have been theoretically predicted, but there is still a controversy on whether the mean-field description used on those models could sweep under the carpet part of the relevant physics which would destroy the time crystalline order. Part of the controversy is related to the fact that there is no well-posed description of what an *open system* time-crystal should be.

In this work we propose plausible criteria to define and characterize discrete time crystals in open systems governed by a Lindblad master equation. Our study is based on the analysis of the so-called Floquet propagator and the properties the associated Liouvillian must have in order to support time crystallinity. Further, we investigate the stability mechanisms and analyze how time crystals can be implemented in open systems. Also, there has been some discussion around the possibility that only *long-range* models can exhibit time crystalline order in open quantum systems. Only very recently, the possibility of having time crystals in an open Ising model have been discussed [26]. Our analysis shows that long-range interactions (or mean-field models) are not crucial features to observe time-crystalline behavior. Nonetheless, our findings show that *long-range* jump operators are relevant in order to have subharmonic oscillations that are more robust to errors.

The outline of the article is as follows: In Sec. 2, we present in detail the most relevant tools and concepts used throughout. In Sec. 3, we introduce the definition of time crystals in open systems and derive some important properties to further characterize them. In section Sec. 4, a collection of low dimensional open system examples is introduced in order to build up some intuition on how to reach stability of time crystals. Sec. 5 and Sec. 6 form the main body of this work, there we present a short range many-body model (XY model) and evaluate its properties and validity as an open system time crystal using the definitions proposed in Sec. 3. To this aim we derive its corresponding master equation and solve it numerically. Finally we present our conclusions.

2 Open quantum system dynamics: concepts and tools

In this section, we introduce the tools of –Markovian– open quantum systems and fix the notation used throughout the article. In what it follows, \mathcal{H} denotes a Hilbert space of dimension $d_{\mathcal{H}}$, $\text{Op}(\mathcal{H})$ denotes the set of operators acting on \mathcal{H} and $\text{S}(\mathcal{H}) \subset \text{Op}(\mathcal{H})$ the set of states. Also, $\text{SOp}(\mathcal{H})$ denotes the set of all *superoperators* i.e., all linear maps between elements of $\text{Op}(\mathcal{H})$.

2.1 Open systems dynamics

Consider a closed time-independent physical system whose dynamics is generated by a Hamiltonian $\mathbf{H} \in \text{Op}(\mathcal{H})$. Then, the Schrödinger equation:

$$\partial_t |\Phi\rangle = -i\mathbf{H}|\Phi\rangle \rightarrow |\Phi(t)\rangle = e^{-i\mathbf{H}t} |\Phi(0)\rangle, \quad (1)$$

and the state $|\Phi\rangle$ undergoes unitary dynamics. Often, one is interested only on the dynamics of a reduced set of the degrees of freedom commonly referred to as *system* (S). Complementary to those, there are *bath* (B) or *environment* degrees of freedom. A partition $\mathbf{H} = \mathbf{H}_S + \mathbf{H}_{SB} + \mathbf{H}_B$ is always possible, where the subscript indicates the degrees of freedom of the system (S), the bath (B) or both at the same time (SB). The Markovian evolution of a reduced system S is generated by the so-called Lindblad master equation:

$$\partial_t \rho = \mathcal{L}\rho = -i[\mathbf{H}_S, \rho] + \sum_{\alpha} \left(\mathbf{L}^{\alpha} \rho \mathbf{L}^{\alpha\dagger} - \frac{1}{2} \{ \mathbf{L}^{\alpha\dagger} \mathbf{L}^{\alpha}, \rho \} \right). \quad (2)$$

where \mathcal{L} denotes the *Liouvillian* superoperator and \mathbf{L}^{α} are the jump operators. When the state of the system is initially uncorrelated from that of the environment, Eq. (2) can be derived from Eq. (1) under three key approximations [27, 28]: the coupling between the system and the environment is weak (weak-coupling approximation), and the environment equilibrates fast (Markov approximation). In addition, the fast rotating terms are usually disregarded (secular approximation). Note that Eq. (2) is a hermiticity preserving equation, i.e., $\mathcal{L}\rho^{\dagger} = (\mathcal{L}\rho)^{\dagger}$. Such evolution generates a family of completely-positive and trace-preserving (CPTP) maps satisfying $\mathcal{E}(t+s) = \mathcal{E}(t) \circ \mathcal{E}(s)$ and $\mathcal{E}(0) = \mathcal{I}$, where \mathcal{I} is the identity map. Remarkably, different Lindblad equations can give rise to the same CPTP map. For instance, Eq. (2) is invariant under the *gauge* transformation, for $a \in \mathbb{C}$,

$$\begin{aligned} \mathbf{H}_S &\mapsto \mathbf{H}'_S = \mathbf{H}_S - \frac{i}{2} (a^* \mathbf{L}^{\alpha} - a \mathbf{L}^{\alpha\dagger}), \\ \mathbf{L}^{\alpha} &\mapsto \mathbf{L}'^{\alpha} = \mathbf{L}^{\alpha} + a \mathbf{1}. \end{aligned} \quad (3)$$

Since linear operators form a vector space, a useful tool to characterize operators is the so-called vectorization procedure that maps any linear operator to a vector, i.e., $\mathbf{O} = \sum_{ij} \mathbf{O}_{ij} |i\rangle \langle j| \in \text{Op}(\mathcal{H}) \mapsto |\mathbf{O}\rangle\rangle = \sum_{ij} \mathbf{O}_{ij} |i\rangle \otimes |j\rangle^* \in \mathcal{H} \otimes \mathcal{H}$. Accordingly, $\mathbf{X}\mathbf{O}\mathbf{Y} \mapsto \mathbf{X} \otimes \mathbf{Y}^T |\mathbf{O}\rangle\rangle$. The same transformation holds for linear superoperators, being now regular operators on $\mathcal{H} \otimes \mathcal{H}$. In an abuse of notation, we denote with the same symbol both, $\mathcal{O} \in \text{SOp}(\mathcal{H})$ and $\mathcal{O} \in \text{Op}(\mathcal{H} \otimes \mathcal{H})$. The inner product in the extended Hilbert space is given by the Hilbert-Schmidt product defined by $\langle\langle \mathbf{X} | \mathbf{Y} \rangle\rangle = \text{tr} [\mathbf{X}^{\dagger} \mathbf{Y}]$. It automatically introduces the notion of *adjoint* superoperator fulfilling

$$\langle\langle \mathbf{X} | \mathcal{O} \mathbf{Y} \rangle\rangle = \text{tr} [\mathbf{X}^{\dagger} \mathcal{O} \mathbf{Y}] = \text{tr} [(\mathcal{O}^{\ddagger} \mathbf{X})^{\dagger} \mathbf{Y}] = \langle\langle \mathcal{O}^{\ddagger} \mathbf{X} | \mathbf{Y} \rangle\rangle, \quad (4)$$

with the property $\mathcal{O} = \mathbf{X} \cdot \mathbf{Y} \Rightarrow \mathcal{O}^{\ddagger} = \mathbf{X}^{\dagger} \cdot \mathbf{Y}^{\dagger}$. In particular, the adjoint Lindblad equation yields

$$\mathcal{L}^{\ddagger} \mathbf{O} = i[\mathbf{H}_S, \mathbf{O}] + \sum_{\alpha} \left(\mathbf{L}^{\alpha\dagger} [\mathbf{O}, \mathbf{L}^{\alpha}] + [\mathbf{L}^{\alpha\dagger}, \mathbf{O}] \mathbf{L}^{\alpha} \right). \quad (5)$$

Using the vectorization procedure, \mathcal{L} admits a matrix representation of dimension $d_{\mathcal{H}}^2 \times d_{\mathcal{H}}^2$. Hence, there is a set of $d_{\mathcal{H}}^2$ eigenvalues $\{\lambda_{\mu}\}$ that can be found as the roots of the

characteristic polynomial $P_{\mathcal{L}}(\lambda) = \det(\mathcal{L} - \lambda\mathcal{I})$. The ordinary *left* and *right* eigenvectors are defined as non-trivial solutions of the equations

$$\begin{aligned}\mathcal{L}^\dagger |\mathbf{l}_\mu\rangle\rangle &= \lambda_\mu^* |\mathbf{l}_\mu\rangle\rangle, \\ \mathcal{L} |\mathbf{r}_\mu\rangle\rangle &= \lambda_\mu |\mathbf{r}_\mu\rangle\rangle.\end{aligned}\tag{6}$$

In the following, we outline some important mathematical properties of \mathcal{L} that will be needed later. For simplicity, we assume that \mathcal{L} is diagonalizable and refer the reader to App. A and references [27, 29–31] for an extended discussion.

- (i) The eigenvalues of \mathcal{L} are either real or come by conjugate pairs. Also, positivity requires the eigenvalues to have negative real part $\text{Re}\lambda_\mu \leq 0$.
- (ii) Ordinary eigenvectors of different eigenvalue are linearly independent.
- (iii) The ordinary eigenvectors of \mathcal{L} and \mathcal{L}^\dagger can be chosen bi-orthogonal, i.e. $\langle\langle \mathbf{l}_\mu | \mathbf{r}_\nu \rangle\rangle = \delta_{\mu\nu}$. More compactly, for diagonalizable \mathcal{L} we have $\mathcal{W}_l^\dagger \mathcal{W}_r = \mathcal{I}$, where the columns of \mathcal{W}_r are the right eigenvectors $|\mathbf{r}_\mu\rangle\rangle$ (and similarly for \mathcal{W}_l).
- (iv) For $t \geq 0$, the solution of Eq. (2) for an initial state $\rho(0)$ is given by $\rho(t) = \mathcal{E}(t)\rho(0)$, where

$$\mathcal{E}(t) = \mathcal{T} \exp\left(\int_0^t ds \mathcal{L}(s)\right),\tag{7}$$

where we allow for time-dependent generator $\mathcal{L}(t)$, and the symbol \mathcal{T} stands for the time-ordering operator.

- (v) For any \mathcal{L} there is always one eigenvalue $\lambda_0 = 0$, with left eigenvector $\langle\langle \mathbf{1} |$. The corresponding right eigenvector $\rho_\infty = \mathbf{r}_0$ fulfills $\mathcal{E}(t)\rho_\infty = \rho_\infty$ and is often referred to as the steady-state. The steady-state might not be unique.

Since the steady-state may not be unique, it is useful to introduce the asymptotic subspace:

$$\text{As}(\mathcal{H}) = \text{span}\{\mathbf{r}_\mu \in \text{Op}(\mathcal{H}) : \text{Re}\lambda_\mu = 0\}.\tag{8}$$

In some contexts, the set of eigenvalues associated to the asymptotic subspace are also called the *peripheral spectrum*. Note that the elements $\mathbf{r}_\mu \in \text{As}(\mathcal{H})$ are general elements of $\text{Op}(\mathcal{H})$ and not always proper quantum states. Also, they are not always steady, but rather non-decaying. The asymptotic space can be always diagonalized, otherwise the dynamics will explode as $t \rightarrow \infty$ (see for instance [32]). From now on, we denote the elements of the asymptotic space by $\Psi_\mu \in \text{As}(\mathcal{H})$ and we just refer to the orthogonal projection as the decay space (see Fig.1). We also define the *dissipative gap* Δ as:

$$\Delta := \min_{\mu} |\text{Re}\lambda_\mu| \quad \text{such that} \quad \text{Re}\lambda_\mu \neq 0,\tag{9}$$

that fixes the time-scale of convergence towards the steady state of the system.

2.2 Conserved quantities of the evolution

In closed systems, any symmetry of the Hamiltonian is a conserved quantity of the evolution. In dissipative systems, this is not always the case, and the relation between symmetries and conserved quantities is, in general, more complex. Here we formulate a simplification of the correspondence between steady-states and conserved quantities presented

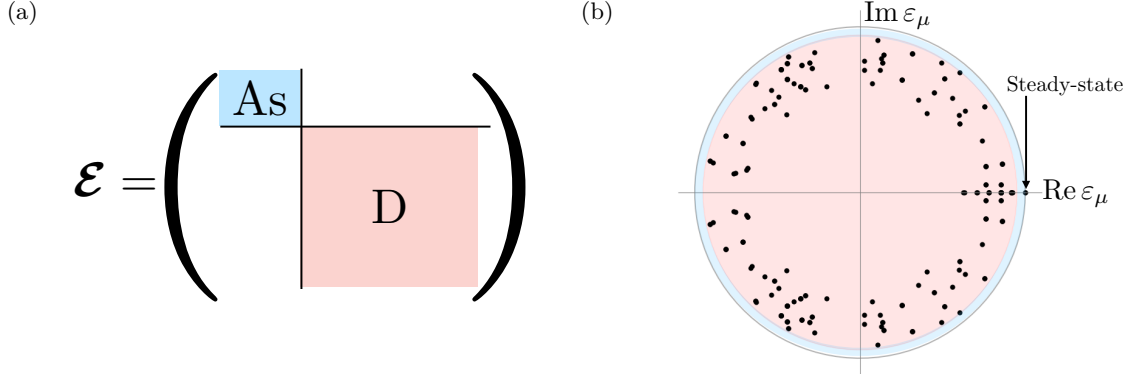


Figure 1: (a) Schematic decomposition of $\mathcal{H} \otimes \mathcal{H}$ in terms of the asymptotic (blue) and decay (red) spaces. (b) Typical spectrum of a CPTP map where the peripheral spectrum is colored in blue and the decaying states in red.

in [33]: Basically, given $|\Psi_\mu\rangle\rangle$, the eigenvectors of \mathcal{L} spanning $\text{As}(\mathcal{H})$ with eigenvalues $\lambda_\mu = i\omega_\mu$, there is a corresponding set of conserved quantities $\langle\langle \mathbf{j}_\mu |$ such that, for any initial state $|\rho(0)\rangle\rangle$, asymptotically we have

$$|\rho(t)\rangle\rangle = \sum_{\mu} e^{i\omega_\mu t} \langle\langle \mathbf{j}_\mu | \rho(0) \rangle\rangle |\Psi_\mu\rangle\rangle + \mathcal{O}(e^{-\Delta t}) \quad (10)$$

where $\langle\langle \mathbf{j}_\mu | \rho(0) \rangle\rangle$ is the imprint of the initial state on the conserved quantities. For instance, when there is only one steady-state, $\langle\langle \mathbf{j}_0 | = \langle\langle \mathbf{1} |$ is the only conserved quantity and the trace $\text{tr}[\rho(0)]$ is conserved throughout the evolution. An analytic expression for the conserved quantities that we will use throughout Sec. 4 was given in [33].

2.3 Periodic time-dependent Hamiltonians in open systems

When the Hamiltonian depends parametrically on time, i.e., $\mathbf{H} \mapsto \mathbf{H}(t)$, the dynamics is governed by the unitary operator

$$\mathbf{U}(t, t_0) = \mathcal{T} \exp \left(-i \int_{t_0}^t ds \mathbf{H}(s) \right). \quad (11)$$

Solving the dynamics of arbitrarily driven time-dependent systems is, in general, quite demanding. The situation can be simplified if we allow the Hamiltonian to have a symmetry in time $\mathbf{H}(t+T) = \mathbf{H}(t)$. For this type of systems, the generator of the evolution over one period, namely $\mathbf{U}(t_0+T, t_0)$ can be used to study the stroboscopic evolution of the system, i.e., at times $t = t_0 + nT$. The initial time t_0 can be regarded as a *gauge* freedom and we will set it to $t_0 = 0$ by convenience. We define $\mathbf{U}_F = \mathbf{U}(T, 0)$ as the Floquet generator, which will be of crucial importance in this work.

Studying the reduced dynamics of the system, requires further tracing out the bath degrees of freedom. As a first approach to periodic driven-dissipative dynamics, we focus on a class of driving protocols for which this operation is analytically doable: the *kicked* protocols. Consider a constant system-bath Hamiltonian \mathbf{H}_1 , which we kick periodically with with a Hamiltonian \mathbf{H}_K that only contains system degrees of freedom. More precisely,

$$\mathbf{H}(t) = \mathbf{H}(t+T) = \mathbf{H}_1 + g \sum_m \delta(t - mT) \mathbf{H}_K. \quad (12)$$

The stroboscopic evolution of the full system-bath is governed by the Floquet propagator $\mathbf{U}_F = \exp(-ig\mathbf{H}_K) \exp(-i\mathbf{H}_1 T)$. Hence, the state of the system after one period is given:

$$\rho(T) = \mathbf{U}_{K\text{trB}} [\exp(-i\mathbf{H}_1 T) \rho(0) \otimes \rho_B \exp(i\mathbf{H}_1 T)] \mathbf{U}_K^\dagger = \mathbf{U}_K \mathcal{E}(T) \rho(0) \mathbf{U}_K^\dagger, \quad (13)$$

where $\mathcal{E}(T)$ is the CPTP map giving rise to the static one period evolution, and $\mathbf{U}_K = \exp(-ig\mathbf{H}_K)$ is the unitary kick operator. Therefore, for a kicked open system, we use the dissipation model of the time-independent problem. Note that, the Born approximation guarantees the state of the bath to remain unchanged after one period of the evolution. Therefore, we can iterate this process to obtain the state of the system at stroboscopic times $t = mT$ with $m \in \mathbb{N}$. The kicked protocol is used, for instance, in the models studied in [17, 24, 25].

3 Discrete time crystals beyond closed systems

As discussed in the introduction, time crystals in closed systems are identified by exhibiting: (I) discrete **time-translational symmetry breaking**, (II) **rigidity** on the subharmonic response of the order parameter and (III) the infinite **persistence** of the subharmonic response in the thermodynamic limit. Based in these conditions, we propose to characterize an *open system time crystal* using a single object, the Floquet propagator [17]:

$$\mathcal{E}_F := \mathcal{E}(T) = \mathcal{T} \exp \left(\int_0^T ds \mathcal{L}(s) \right), \quad (14)$$

The spectrum $\{\varepsilon_\mu\}$ of \mathcal{E}_F fully characterizes the stroboscopic properties of periodically driven systems. Note that all ε_μ lie within the unit circle. Focusing on: (i) The asymptotic space that we can now identify $\text{As}(\mathcal{H}) = \text{span} \{ \Psi_\mu \in \text{Op}(\mathcal{H}) : |\varepsilon_\mu| = 1 \}$, i.e., those eigenstates lying on the unit circle; and (ii) the dissipative gap $\Delta_F := \max_\mu \{ 1 - \log |\varepsilon_\mu| : |\varepsilon_\mu| \neq 1 \}$, the identification criteria for an open discrete time crystal can be formulated as:

- (I) **Time-translation symmetry breaking:** there exists at least one $\mu = \mu^*$ for which $\varepsilon_{\mu^*}^N = 1$, but $\varepsilon_{\mu^*} \neq 1$. Note that if $\varepsilon_{\mu^*} \neq -1$ it comes with its conjugate pair.
- (II) **Rigidity of the oscillations:** given a deformation of the protocol $\mathcal{E}_F \mapsto \mathcal{E}_F + \eta \mathcal{V}$, the first order *susceptibility* $\chi^{(1)} = \left| (\partial \varepsilon_{\mu^*} / \partial \eta)_{\eta=0} \right| \ll 1$. This can sometimes be easily computed using perturbation theory: $\chi^{(1)} = \langle \langle \mathbf{1}_{\mu^*} | \mathcal{V} | \mathbf{r}_{\mu^*} \rangle \rangle$, see appendix App. B for details.
- (III) **Persistence to infinite time:** Strictly speaking, this property is ensured by (i). In general, for finite systems, $0 < \varepsilon_{\mu^*}^N \approx 1$ which will fix the decay rate of the oscillations.

A system fulfilling (I)–(III) displays long-lived and robust subharmonic oscillations and therefore it is in a *time-crystal phase*. In the opposite situation, the system will typically arrive to equilibrium reaching the *thermal phase*.

Let us illustrate the typical scenario of a system in the time-crystal phase in the case of period doubling, i.e., $N = 2$. There should be, at least, two robust eigenvalues of \mathcal{E}_F with modulus one such that $\varepsilon_\mu^2 = 1$. We denote them by $\varepsilon_0 = 1$ and $\varepsilon_\pi = -1$. After a (large) number of periods m , the state of the system will be well approximated by

$$\begin{aligned} \rho_\infty^{(2m)} &= \mathcal{E}_F^{2m} \rho(0) \approx c_0 \rho_0 + c_\pi \mathbf{r}_\pi, \\ \rho_\infty^{(2m+1)} &= c_0 \rho_0 + c_\pi e^{i\pi} \mathbf{r}_\pi = c_0 \rho_0 - c_\pi \mathbf{r}_\pi. \end{aligned} \quad (15)$$

The expectation value of the order parameter after m periods will be

$$f(mT) = \sum_{\mu} \varepsilon_{\mu}^m \langle\langle \mathbf{O} | \mathbf{r}_{\mu} \rangle\rangle \langle\langle \mathbf{1}_{\mu} | \rho(0) \rangle\rangle \approx \langle\langle \mathbf{O} | \rho_0 \rangle\rangle + (-)^m \langle\langle \mathbf{O} | \mathbf{r}_{\pi} \rangle\rangle \langle\langle \mathbf{1}_{\pi} | \rho(0) \rangle\rangle, \quad (16)$$

where we have used $\langle\langle \mathbf{1}_0 | \rho(0) \rangle\rangle = \text{tr}[\rho(0)] = 1$. Therefore, we will be able to observe the long-lived subharmonic oscillations if:

- (a) the choice of $\rho(0)$ is such that $\langle\langle \mathbf{1}_{\pi} | \rho(0) \rangle\rangle \neq 0$, i.e., the initial state has some overlap with the π eigenspace, and
- (b) the choice of \mathbf{O} is such that $\langle\langle \mathbf{O} | \mathbf{r}_{\pi} \rangle\rangle \neq 0$, i.e., the order parameter is sensible to the subharmonic oscillations.

3.1 Useful observations for open system time crystals

Before proceeding further, let us remark some general properties of the Floquet propagator for open system time crystals. We focus on the dynamics consisting on a dissipative evolution under \mathcal{L}_1 during a time t_1 followed from a unitary transformation \mathbf{U}_K (kick).

Observation 1 (kicked system propagator)

The Floquet propagator \mathcal{E}_F of a system under a kicked protocol takes the simple form:

$$\mathcal{E}_F = \mathbf{U}_K \otimes \mathbf{U}_K^* \exp(\mathcal{L}_1 t_1), \quad (17)$$

and has always an eigenvalue $\varepsilon_0 = 1$.

Proof It follows from Eq. (14) the form of the Floquet propagator. Notice that

$$\langle\langle \mathbf{1} | \mathcal{E}_F = \left(\exp(\mathcal{L}_1^{\dagger} t_1) \mathbf{U}_K^{\dagger} \otimes \mathbf{U}_K^T | \mathbf{1} \rangle \right)^{\dagger} = \left(\exp(\mathcal{L}_1^{\dagger} t_1) | \mathbf{1} \rangle \right)^{\dagger} = \langle\langle \mathbf{1} |, \quad (18)$$

and therefore $\langle\langle \mathbf{1} | \mathcal{E}_F = \langle\langle \mathbf{1} |$ has eigenvalue 1. Alternatively, it is a consequence of the fact that a concatenation of trace preserving maps is also trace preserving.

Observation 2 (unitarily transformed spectrum)

The spectrum of a CPTP map \mathcal{E} is unchanged under the unitary transformation $\mathcal{U}_K = \mathbf{U}_K \otimes \mathbf{U}_K^*$ corresponding to $\mathcal{E}_F = \mathcal{U}_K \mathcal{E} \mathcal{U}_K^{\dagger}$.

Proof It follows from noting that the characteristic equation is invariant under unitary transformations, i.e., $P_{\mathcal{E}}(\lambda) = (\mathcal{E} - \lambda \mathcal{I}) = \det(\mathcal{E}_F - \lambda \mathcal{I}) = P_{\mathcal{E}_F}(\lambda)$.

Observation 3 (kicked spectrum)

The spectrum of a CPTP map \mathcal{E} is generically changed under a kick $\mathcal{U}_K = \mathbf{U}_K \otimes \mathbf{U}_K^*$ corresponding to $\mathcal{E}_F = \mathcal{U}_K \mathcal{E}$.

Proof The characteristic equation is, in general, not invariant under *one-sided* unitary transformations, i.e., $P_{\mathcal{E}}(\lambda) = (\mathcal{E} - \lambda \mathcal{I}) \neq \det(\mathcal{E}_F - \lambda \mathcal{I}) = P_{\mathcal{E}_F}(\lambda)$.

Observation 4 (asymptotic space of a kicked evolution)

Consider $\{|\psi_k\rangle\}$ and $\{|\phi_k\rangle\}$ two basis of \mathcal{H} and a CPTP map \mathcal{E} . If \mathcal{E} is such that $\mathcal{E} |\psi_k\rangle \langle\psi_{k'}| = |\phi_k\rangle \langle\phi_{k'}|$ for a subset of tuples $(k, k') \in S$, then it exists a unitary kick \mathbf{U}_K such that $\mathcal{E}_F = \mathbf{U}_K \otimes \mathbf{U}_K^* \mathcal{E}$ has at least $|S|$ elements in its asymptotic space.

Proof. Consider the unitary kick $\mathbf{U}_K := \sum_k |\psi_k\rangle \langle\phi_k|$. Then for all $(k, k') \in S$, $\mathcal{E}_F |\psi_k\rangle \langle\psi_{k'}| = |\psi_k\rangle \langle\psi_{k'}|$ and are therefore part of $\text{As}(\mathcal{H})$ of the map \mathcal{E}_F . Note that the combinations of k and k' that form S are not completely arbitrary. Since the map \mathcal{E}

is positive, the tuples (k, k') with $k \neq k'$ can only be part of S if also $(k, k) \in S$ and $(k', k') \in S$.

Remark. Note that, in general, the dimension of the asymptotic space of a CPTP map \mathcal{E} can increase, decrease or stay equal after a unitary kick.

Observation 5 (multistability and time-crystals)

A CPTP Floquet map \mathcal{E}_F supports time crystalline behavior only if $\dim \text{As}(\mathcal{H}) \geq 1$. The converse is not true.

Proof By contradiction, if it exists one and only one eigenstate \mathbf{r}_μ with $|\varepsilon_\mu| = 1$, it corresponds to a normalizable $\rho_\infty = \mathbf{r}_0$, such that $\text{tr}[\rho_\infty] = 1$. Given any initial state $\rho(0)$

$$\lim_{n \rightarrow \infty} \rho(mT) = \lim_{m \rightarrow \infty} \mathcal{E}_F^m \rho(0) = \rho_\infty, \quad (19)$$

which proves that, asymptotically, the state has the same periodicity than the Liouvillian, i.e., $\rho((m+1)T) = \rho(mT)$. The converse implication fails, for instance, when there are two non-decaying states with the same eigenvalue $\varepsilon_{0,1} = \varepsilon_{0,2}$ which implies a T -periodic response even though $\dim \text{As}(\mathcal{H}) \geq 1$.

Observation 6 (general protocol for sub-harmonic response)

A general kicked protocol on a CPTP map \mathcal{E} with a unitary \mathbf{U}_K that gives rise to sub-harmonic response can be obtained by demanding:

- (i) the map \mathcal{E} exhibits static multistability, i.e., the peripheral spectrum contains only eigenvalues $\varepsilon_\mu = 1$.
- (ii) the unitary kick $\mathbf{U}_K = \mathbf{U}_K \otimes \mathbf{U}_K^*$ acts independently on the asymptotic and decay spaces, i.e., $\mathbf{U}_K = \mathbf{U}_{\text{As}} \oplus \mathbf{U}_D$.
- (iii) the unitary kick \mathbf{U}_{As} has eigenvalues $u_\alpha = \exp(in_\alpha 2\pi/N)$ with $n_\alpha \in \mathbb{Z}$, and at least one eigenvalue is different from one.

Proof Let us define $\{\Psi_\mu\}$ a basis of $\text{As}(\mathcal{H})$ of \mathcal{E} . Consider the Floquet map $\mathcal{E}_F = \mathbf{U}_K \otimes \mathbf{U}_K^* \mathcal{E}$. From condition (i) follows $\mathcal{E}_F |\Psi_\mu\rangle\rangle = \mathbf{U}_K |\Psi_\mu\rangle\rangle$. Condition (ii) implies that:

$$\mathcal{E}_F^m |\rho(0)\rangle\rangle = \sum_\mu c_\mu \mathbf{U}_{\text{As}}^m |\Psi_\mu\rangle\rangle + \mathcal{O}(e^{-\Delta m T}), \quad (20)$$

where $c_\mu = \langle\langle \mathbf{j}_\mu | \rho(0) \rangle\rangle$ and $\langle\langle \mathbf{j}_\mu |$ the associated conserved quantities to $|\Psi_\mu\rangle\rangle$. Finally, for large enough m , condition (iii) implies that exists an \mathbf{O} such that $f(T) \neq f(0) = f(NT)$.

4 Exemplary: Few-body systems

As previously shown, the structure of the asymptotic subspace $\text{As}(\mathcal{H})$ is crucial to identify when a physical system can support subharmonic response. Here, to gather some intuition, we present a collection of one and two qubit models (specified by \mathbf{H}_S and \mathbf{L}^α) that give rise to different multistable structures of $\text{As}(\mathcal{H})$. However, we do not refer to them as time-crystals since this multistability will be, in general, fine tuned.

4.1 A single qubit: Dephasing

A well known example of dissipative evolution supporting more than one steady state is *pure dephasing*. In this scenario, $\text{As}(\mathcal{H})$ contains the information encoded in the diagonal elements of the initial state (i.e., is able to support only one bit of classical information). We consider:

$$\mathbf{H}_S = \frac{h}{2}\mathbf{Z}, \quad \& \quad \mathbf{L} = \sqrt{\kappa}\mathbf{Z}, \quad (21)$$

where \mathbf{Z} is the z -Pauli matrix. has $\dim \text{As}(\mathcal{H}) = 2$, and $\text{As}(\mathcal{H}) = \text{span}(\mathbf{1}, \mathbf{Z})$ both with eigenvalue $\lambda_\mu = 0$. Note that there are two conserved quantities in this evolution, dual to the two steady states, that can be written as $\mathbf{j}_0 = \mathbf{1}$ and $\mathbf{j}_1 = \mathbf{Z}$. Equivalently, one may think about alternative conserved quantities and steady states $\Psi_\mu = \mathbf{j}_\mu = |\mu\rangle \langle \mu|$ with $\mu = 0, 1$. Consider now $\mathbf{U}_K = \mathbf{X}$, being \mathbf{X} the x -Pauli matrix. This can be implemented, for instance, as:

$$\mathbf{H}_S \mapsto \mathbf{H}_S(t) = \frac{h}{2}\mathbf{Z} + \pi \sum_n \delta(t - nT) \frac{\mathbf{X}}{2}. \quad (22)$$

such that $\mathbf{H}_S(t + T) = \mathbf{H}_S(t)$. Then $\mathcal{E}_F = \mathbf{X} \otimes \mathbf{X} \exp(\mathcal{L}T)$ with the spectrum:

$$\{\epsilon_\mu\} = \{1, -1, e^{-2\kappa T}, -e^{-2\kappa T}\}. \quad (23)$$

The basis of $\text{As}(\mathcal{H})$ for \mathcal{E}_F is again given by $\Psi_\mu = |0\rangle \langle 0| + (-)^\mu |1\rangle \langle 1|$ fulfilling $\mathcal{E}_F \Psi_\mu = (-)^\mu \Psi_\mu$ with $\mu = 0, 1$.

Then, if we take $\rho(0) = p|0\rangle \langle 0| + (1-p)|1\rangle \langle 1|$, the evolved state will be $\rho_\infty(nT) = p|0 \oplus n\rangle \langle 0 \oplus n| + (1-p)|1 \oplus n\rangle \langle 1 \oplus n|$, giving rise to subharmonic oscillations in the magnetization of amplitude $2p - 1$. Hence, for such a protocol, criteria (I) of Sec. 3 is fulfilled. The next question is, of course, whether or not these oscillations are robust under perturbations, i.e., if criteria (II) is also fulfilled.

For simplicity consider the case $h = 0$. This protocol is not robust to adding a perpendicular Hamiltonian since the deformation $\mathbf{H}_S \mapsto \mathbf{H}_S(\eta) = \mathbf{H}_S + \eta\mathbf{X}/2$ opens a linear gap in the Liouvillian spectrum of Eq. (21)

$$\begin{aligned} \{\lambda_\mu\} &= \left\{ 0, -\kappa + \sqrt{\kappa^2 - \eta^2}, -\kappa - \sqrt{\kappa^2 - \eta^2}, -2\kappa \right\} \\ &\approx \left\{ 0, -\frac{\eta}{2}, -2\kappa + \frac{\eta}{2}, -2\kappa \right\} + \mathcal{O}(\eta^2), \end{aligned} \quad (24)$$

and bistability is lost. Since $\chi^{(1)} = 1/2 \not\ll 1$, we see that condition (II) is not fulfilled. Instead, consider the deformation of committing an error in the rotation angle:

$$\mathbf{H}_S(t) \mapsto \mathbf{H}_S(\eta, t) = (\pi + \eta) \sum_n \delta(t - nT) \frac{\mathbf{X}}{2}, \quad (25)$$

which corresponds to $\mathcal{V}(\cdot) = -i/2[\mathbf{X}, \mathcal{E}_F(\cdot)]$. The spectrum of $\mathcal{E}_F(\eta)$, to lowest order in η , is given by

$$\{\epsilon_\mu\} = \left\{ 1, -1 + \frac{1}{2} \coth(\kappa T) \eta^2, e^{-2\kappa T}, -e^{-2\kappa T} \left(1 + \frac{1}{2} \coth(\kappa T) \eta^2 \right) \right\} + \mathcal{O}(\eta^3). \quad (26)$$

which yields $\chi^{(1)} = 0$ and makes the subharmonic response linearly robust to rotation errors.

4.2 Two qubits: Local jumps

We have studied a one-qubit scenario where $\text{As}(\mathcal{H})$ could support one classical bit. In this subsection, we consider the larger Hilbert space of two two level systems $\mathcal{H} = \mathbb{C}^2 \otimes \mathbb{C}^2$. A new structure of $\dim \text{As}(\mathcal{H})$ that supports quantum information (i.e., the information contained in the coherences) can now arise. These instances of asymptotic space are known as *decoherence free subspaces* and have been recently studied in the literature as dissipation protected memories (see for instance [32, 34–36]). We examine different subcases, and focus on the differences between those. For convenience, we also introduce the Bell basis:

$$\begin{aligned} |\psi_\alpha\rangle &= \frac{|01\rangle + (-)^\alpha |10\rangle}{\sqrt{2}} \\ |\phi_\alpha\rangle &= \frac{|00\rangle + (-)^\alpha |11\rangle}{\sqrt{2}}, \end{aligned} \quad (27)$$

We consider first the case of no Hamiltonian but *local* noise operators:

$$\mathbf{H}_S = 0, \quad \& \quad \mathbf{L}^\alpha = |\psi_\alpha\rangle \langle \phi_\alpha|. \quad (28)$$

It is easy to see that $\text{As}(\mathcal{H}) = \text{span}(\Psi_{\alpha\beta})$ with $\Psi_{\alpha\beta} = |\psi_\alpha\rangle \langle \psi_\beta|$ and, therefore, $\dim \text{As}(\mathcal{H}) = 4$. Note that we can encode the state of a qubit inside $\text{As}(\mathcal{H})$ and it will be protected from dissipation. The conserved quantities read [33]

$$\mathbf{j}_{\alpha\beta} = |\psi_\alpha\rangle \langle \psi_\beta| + \delta_{\alpha\beta} |\phi_\alpha\rangle \langle \phi_\beta|, \quad (29)$$

for $\alpha, \beta = 0, 1$. Two of those four conserved quantities correspond to the populations of $\alpha = \beta = 0$ and $\alpha = \beta = 1$, while the other two $\alpha \neq \beta$ correspond to the coherences only within the ψ -block. The coherences in the ϕ -space are destroyed by dissipation.

4.3 Two qubits: Collective jumps

If now we consider a *collective* noise operator $\mathbf{L} = \sum_\alpha \mathbf{L}^\alpha = \sum_\alpha |\psi_\alpha\rangle \langle \phi_\alpha|$, the same asymptotic space $\text{As}(\mathcal{H}) = \text{span}(|\psi_\alpha\rangle \langle \psi_\beta|)$ is found. The key difference can be spotted by looking at the conserved quantities. We encounter

$$\mathbf{j}_{\alpha\beta} = |\psi_\alpha\rangle \langle \psi_\beta| + |\phi_\alpha\rangle \langle \phi_\beta|, \quad (30)$$

and therefore, also the coherences within the ϕ -space are now preserved. It turns out that preserving the coherences will become crucial in order to construct robust time-crystals.

4.4 Two qubits: Coherence suppression by a jump

We now look at the effect of the decay operators within the ϕ -space. Consider a jump $\mathbf{L}(\eta) = \sum_\alpha |\psi_\alpha\rangle \langle \phi_\alpha| + \eta \vec{n} \cdot \vec{\sigma}_\phi$, where \vec{n} is the Bloch vector and $\vec{\sigma}_\phi$ is the Pauli vector in the ϕ subspace (e.g. $\vec{\sigma}_\phi^3 = \sum_\alpha (-)^\alpha |\phi_\alpha\rangle \langle \phi_\alpha|$). This gives rise to a suppression factor for the coherences that depends on the particular choice of \vec{n} . In general,

$$\mathbf{j}_{\alpha\beta} = |\psi_\alpha\rangle \langle \phi_\beta| + \frac{|\eta|^2}{1 + 2|\eta|^2} (\vec{n} \cdot \vec{\sigma}_\phi) |\phi_\alpha\rangle \langle \phi_\beta| (\vec{n} \cdot \vec{\sigma}_\phi) + \frac{1 + |\eta|^2}{1 + 2|\eta|^2} |\phi_\alpha\rangle \langle \phi_\beta|. \quad (31)$$

For instance, the particular choice of $\vec{n} = (0, 0, 1)$ leads to

$$\mathbf{j}_{\alpha\beta} = |\psi_\alpha\rangle \langle \psi_\beta| + \frac{1 + |\eta|^2(1 + (-)^{\alpha+\beta})}{1 + 2|\eta|^2} |\phi_\alpha\rangle \langle \phi_\beta|, \quad (32)$$

which indicates that dephasing within the decay space is translated into a coherence suppression of order $\sim |\eta|^{-2}$ within the ϕ -block.

4.5 Two qubits: Coherence suppression by a Hamiltonian

Finally, we will look at the effect of having a Hamiltonian that acts locally in the ψ and ϕ subspaces. This translates into having residual Hamiltonian evolution in the steady-state. Consider,

$$\mathbf{H}_S = \frac{h}{2}\mathbf{Z}_\psi + \frac{h + \delta}{2}\mathbf{Z}_\phi, \quad (33)$$

and $\mathbf{L} = \sum_\alpha |\psi_\alpha\rangle\langle\phi_\alpha|$. The conserved quantities now read

$$\mathbf{j}_{\alpha\beta} = |\psi_\alpha\rangle\langle\psi_\beta| + \frac{|\phi_\alpha\rangle\langle\phi_\beta|}{1 - (-)^\alpha(1 - \delta_{\alpha\beta})i\delta}. \quad (34)$$

Hence, the effect of a coherent evolution within the asymptotic and decay space is to suppress the coherences between the ϕ -block. However, the strength depends on the effective detuning δ between the two spaces.

Now, we have several possibilities of jumps operators, all of them giving rise to the same $\text{As}(\mathcal{H})$ but with different conserved quantities and different eigenvalues λ_μ . Regardless of the one we chose, a TC protocol can be implemented by kicking the system periodically with the rotation $\mathbf{U}_K = \mathbf{X}_\psi + \mathbf{X}_\phi$. Note that $\mathbf{U}_K^2 = \mathbf{1}$ and $\mathbf{u}_K = \mathbf{u}_{\text{As}} \oplus \mathbf{u}_\perp$, giving rise to subharmonic response for $N = 2$. It can be implemented by:

$$\mathbf{H}_S(t) = \frac{\pi}{2} \sum_n \delta(t - nT)(\mathbf{X}_\psi + \mathbf{X}_\phi). \quad (35)$$

For \mathcal{E}_F , the asymptotic space is $\text{As}(\mathcal{H}) = \text{span}(\tilde{\Psi}_{\alpha\beta})$, with

$$\tilde{\Psi}_{\alpha\beta} = \frac{\Psi_{00} + (-)^{\alpha+\beta}\Psi_{11} + (-)^\alpha\Psi_{10} + (-)^\beta\Psi_{01}}{2}, \quad (36)$$

with eigenvalues $\varepsilon_{\alpha\beta} = (-1)^{\alpha+\beta}$. The same linear combination gives rise to the conserved quantities $\tilde{\mathbf{j}}_{\alpha\beta}$. The order parameter \mathbf{O} can be any observable that does not transform trivially under the *not*-gate \mathbf{X}_ψ , e.g., $\mathbf{O} = \mathbf{Z}_\psi$ fulfilling $\mathbf{X}_\psi\mathbf{Z}_\psi\mathbf{X}_\psi = -\mathbf{Z}_\psi$. In the local basis, this looks like $\mathbf{O} = |01\rangle\langle 10| + |10\rangle\langle 01|$ which is a coherence measure between the excitation of the two qubits. Hence, condition (I) is fulfilled. Regarding condition (II), exact diagonalization of the perturbed protocol is, in general, analytically demanding. However, if an error η is made in the rotation angle, that is $\mathcal{V}(\cdot) = -i[\mathbf{X}_\psi + \mathbf{X}_\phi, \mathcal{E}_F(\cdot)]$, the susceptibility can be computed. Using perturbation theory, one can verify $\chi^{(1)} = \langle\langle \tilde{\mathbf{j}}_{\alpha\beta} | \mathcal{V} | \tilde{\Psi}_{\alpha\beta} \rangle\rangle = i(-)^\alpha(1 - \delta_{\alpha\beta})$. In fact, this particular case can be computed at all orders to see that the spectrum for any η is $\{\varepsilon_{\alpha\beta}\} = \{1, 1, -e^{i\eta}, -e^{-i\eta}\}$. A similar calculation, but with the generator of the kick operator given by $\mathbf{M}_x = \mathbf{X}_0 + \mathbf{X}_1$, shows instead a robust rotation (i.e. $\chi^{(1)} = 0$). This last case, can be mapped to an open Ising chain of 2 particles that are kicked with the total magnetization \mathbf{M}_x along the x -direction.

5 The XY time-crystal

Keeping in mind the results obtained so far for low dimensional systems, we focus here in the *short-range* XY chain. First, we derive the master equation governing the dynamics of the XY model coupled to the environment and second, we analyze if a time-crystal is possible in such a system.

5.1 The open XY model

Consider a system described by the Hamiltonian:

$$\mathbf{H}_\xi = -J \sum_{r=1}^L \left(\frac{1+\gamma}{2} \mathbf{X}_r \mathbf{X}_{r+1} + \frac{1-\gamma}{2} \mathbf{Y}_r \mathbf{Y}_{r+1} + h \mathbf{Z}_r \right), \quad (37)$$

representing a 1D lattice of L spins that interact anisotropically. We impose periodic boundary conditions (i.e. $\sigma_r = \sigma_{L+r}$, where σ is any pauli matrix \mathbf{X} , \mathbf{Y} or \mathbf{Z}), restrict ourselves to L even, and gather the Hamiltonian parameters as $\xi = (J, \gamma, h)$. This model has several symmetries[37]: (i) a rotation by $\pi/2$ along the z-axis interchanges the x and y spin interactions and it is equivalent to $\gamma \leftrightarrow -\gamma$, (ii) a reflection of the spins with respect to the x-y plane is equivalent to $h \leftrightarrow -h$. Hence, it is sufficient to study the phase diagram for $\gamma, h \geq 0$. It is well known that this system undergoes a quantum phase transition at $h = 1$, that goes from an ordered phase for $h < 1$ to a disordered phase for $h > 1$. The full Hamiltonian of system and bath is given by:

$$\begin{aligned} \mathbf{H} &= \mathbf{H}_\xi + \mathbf{H}_{\text{SB}} + \mathbf{H}_{\text{B}}, \\ \mathbf{H}_{\text{SB}} &= \eta \mathbf{M}_z \otimes \mathbf{B} := \eta \sum_{k,\mu} \sum_{r=1}^N \mathbf{Z}_r \otimes (g_{k,\mu} \mathbf{b}_{k,\mu}^\dagger + g_{k,\mu}^* \mathbf{b}_{k,\mu}), \\ \mathbf{H}_{\text{B}} &= \sum_{k,\mu} \omega_{k,\mu} (\mathbf{b}_{k,\mu}^\dagger \mathbf{b}_{k,\mu} + 1/2), \end{aligned} \quad (38)$$

where k labels the potentially multiple reservoirs and $\eta \ll 1$ is a small parameter ensuring the weak coupling limit. A similar system-bath Hamiltonian was used in [38] to study transport properties. The first step towards the derivation of the master equation is diagonalizing \mathbf{H}_ξ . This can be achieved using the Jordan-Wigner, Fourier and Bogoliubov transformation [37, 39, 40]. In the following, we sketch the diagonalization procedure both for completeness and to fix the notation used subsequently. First we note that \mathbf{H}_ξ can be broken in parity sectors since $[\mathbf{P}, \mathbf{H}_\xi] = 0$ and $\mathbf{P} = \prod_r \mathbf{Z}_r$ with possible eigenvalues $p = \pm 1$. With the Jordan-Wigner transformation, we map spins into fermions using:

$$\mathbf{Z}_s \leftrightarrow 1 - 2\mathbf{c}_s^\dagger \mathbf{c}_s \quad \& \quad \sigma_s^+ \leftrightarrow \exp\left(i\pi \sum_{r<s} \mathbf{c}_r^\dagger \mathbf{c}_r\right) \mathbf{c}_s. \quad (39)$$

Note that this transformation does not depend on ξ . After some manipulation and imposing the appropriate boundary conditions in each parity sector we find:

$$\mathbf{H}_\xi^\pm = -J \sum_{r=1}^L \left(\mathbf{c}_r^\dagger \mathbf{c}_{r+1} + \gamma \mathbf{c}_r^\dagger \mathbf{c}_{r+1}^\dagger - h \mathbf{c}_r^\dagger \mathbf{c}_r + \text{h.c.} \right) - JhL. \quad (40)$$

We now take advantage of the fact that \mathbf{H}_ξ^\pm are translationally invariant and perform the Fourier transform

$$\mathbf{c}_r = \frac{e^{i\pi/4}}{\sqrt{L}} \sum_{q \in \text{BZ}_\pm} e^{i\frac{2\pi}{L}qr} \mathbf{c}_q \quad \& \quad \mathbf{c}_q = \frac{e^{-i\pi/4}}{\sqrt{L}} \sum_{r=1}^L e^{-i\frac{2\pi}{L}qr} \mathbf{c}_r. \quad (41)$$

where BZ_\pm stands for the Brillouin zone specified by:

$$\begin{aligned} \text{BZ}_+ &= \left\{ q = m + \frac{1}{2} \quad m \in \{-L/2, \dots, L/2 - 1\} \right\} && \text{for } \mathbf{H}_\xi^+, \\ \text{BZ}_- &= \left\{ q = \pm m \quad m \in \{-L/2, \dots, L/2 - 1\} \right\} && \text{for } \mathbf{H}_\xi^-. \end{aligned} \quad (42)$$

This brings the Hamiltonian to the explicit block quadratic form

$$\begin{aligned}\mathbf{H}_\xi^\pm &= J \sum_{q \in \text{BZ}_\pm} \begin{pmatrix} \mathbf{c}_q^\dagger & \mathbf{c}_{-q} \end{pmatrix} \begin{pmatrix} h - \cos(\frac{2\pi}{L}q) & -\gamma \sin(\frac{2\pi}{L}q) \\ -\gamma \sin(\frac{2\pi}{L}q) & \cos(\frac{2\pi}{L}q) - h \end{pmatrix} \begin{pmatrix} \mathbf{c}_q \\ \mathbf{c}_{-q}^\dagger \end{pmatrix}, \\ &:= \sum_{q \in \text{BZ}_\pm} \begin{pmatrix} \mathbf{c}_q^\dagger & \mathbf{c}_{-q} \end{pmatrix} \mathbf{H}_{\xi,q} \begin{pmatrix} \mathbf{c}_q \\ \mathbf{c}_{-q}^\dagger \end{pmatrix}.\end{aligned}\quad (43)$$

We can now perform the ξ -dependent Bogoliubov transformation to diagonalize \mathbf{H}_ξ^\pm . Since the matrix $\mathbf{H}_{\xi,q}$ is a combination of the Pauli matrices in the x and z directions, it can be diagonalized via a rotation

$$\mathbf{R}_{\xi,q} = \exp\left(-i\frac{\theta_{\xi,q}}{2}\sigma_y\right) = \begin{pmatrix} \cos\frac{\theta_{\xi,q}}{2} & -\sin\frac{\theta_{\xi,q}}{2} \\ \sin\frac{\theta_{\xi,q}}{2} & \cos\frac{\theta_{\xi,q}}{2} \end{pmatrix}, \quad (44)$$

such that $\tilde{\mathbf{H}}_{\xi,q} = \mathbf{R}_{\xi,q}\mathbf{H}_{\xi,q}\mathbf{R}_{\xi,q}^\dagger$ is diagonal. Setting the off-diagonal terms to zero requires:

$$\theta_{\xi,q} = \tan^{-1} \frac{\gamma \sin\left(\frac{2\pi}{N}q\right)}{h - \cos\left(\frac{2\pi}{N}q\right)}. \quad (45)$$

Finally, the Hamiltonian takes the expression:

$$\mathbf{H}_\xi^\pm = \frac{1}{2} \sum_{q \in \text{BZ}_\pm} \omega_{\xi,q} \left(\mathbf{d}_{\xi,q}^\dagger \mathbf{d}_{\xi,q} - \mathbf{d}_{\xi,-q} \mathbf{d}_{\xi,-q}^\dagger \right) = \sum_{q \in \text{BZ}_\pm} \omega_{\xi,q} (\mathbf{d}_{\xi,q}^\dagger \mathbf{d}_{\xi,q} - 1/2), \quad (46)$$

where \pm stands for the even and odd parity sectors, $\mathbf{d}_{\xi,q}$ are the Bogoliubov fermions and the dispersion is given by:

$$\omega_{\xi,q} = \omega_{\xi,-q} = 2J \sqrt{\left(h - \cos\left(\frac{2\pi}{L}q\right)\right)^2 + \left(\gamma \sin\left(\frac{2\pi}{L}q\right)\right)^2}. \quad (47)$$

Now we are ready to derive the master equation. We sketch here the crucial parts of the derivation, while details are given in App. E. For simplicity we assume only one reservoir, since the extension to multiple baths is straightforward. The starting point is the Redfield equation in the rotating frame of $\mathbf{H}_\xi + \mathbf{H}_B$:

$$\dot{\tilde{\rho}}(t) = - \int_0^\infty d\text{str}_B [\mathbf{H}_{\text{SB}}(t), [\mathbf{H}_{\text{SB}}(t-s), \tilde{\rho}(t) \otimes \rho_{\text{eq}}]]. \quad (48)$$

The jump operators arise from the decomposition of the \mathbf{M}_z into the eigenmodes of the system Hamiltonian. For every quasimomentum q , the magnetization can be divided into three different rotating frequencies with energies labeled by α : $E_{\xi,q}^\alpha = \{0, \pm 2\omega_{\xi,q}\}$ for $\alpha = 0, \uparrow, \downarrow$ respectively. Then, the magnetization can be decomposed as:

$$\mathbf{M}_z(t) = - \sum_{q>0} \sum_{\alpha=0,\uparrow} \mathbf{L}_{\xi,q}^\alpha e^{iE_{\xi,q}^\alpha t}, \quad (49)$$

where $\mathbf{L}_{\xi,q}^0 = 2 \cos \theta_{\xi,q} (\mathbf{d}_{\xi,q}^\dagger \mathbf{d}_{\xi,q} - \mathbf{d}_{\xi,-q} \mathbf{d}_{\xi,-q}^\dagger)$ and $\mathbf{L}_{\xi,q}^\uparrow = 2 \sin \theta_{\xi,q} \mathbf{d}_{\xi,q}^\dagger \mathbf{d}_{\xi,q} = \mathbf{L}_{\xi,q}^{\downarrow\dagger}$. Inserting this expression into Eq. (48), it follows

$$\dot{\tilde{\rho}}(t) = -\eta^2 \sum_{q,q'>0} \sum_{\alpha,\alpha'} \Gamma(E_{\xi,q}^\alpha) e^{-i(E_{\xi,q}^\alpha - E_{\xi,q'}^{\alpha'})t} \left(\mathbf{L}_{\xi,q}^{\alpha\dagger} \mathbf{L}_{\xi,q'}^{\alpha'} \tilde{\rho}(t) - \mathbf{L}_{\xi,q'}^{\alpha'} \tilde{\rho}(t) \mathbf{L}_{\xi,q}^{\alpha\dagger} \right) + \text{h.c.} \quad (50)$$

The next step consists in using the secular approximation, that selects only those terms that fulfill the resonant condition $E_{\xi,q}^\alpha - E_{\xi,q'}^{\alpha'} = 0$. We now see that two different situations arise: in one hand, if ξ is such that the dispersion of the energy as a function of q is approximately flat (e.g., $\gamma = 1$, $h = 0$) the resonant condition gives $\alpha = \alpha'$. If, on the other hand, the dispersion is large enough, only those terms with the same q are resonant. These two conditions lead to collective and local decay processes in the sense of Subsec.4.3. Then, the final master equation for the collective decay processes is given by:

$$\dot{\rho} = -i[\mathbf{H}_\xi, \rho] + \eta^2 \kappa_\xi^\downarrow \left(\mathbf{L}_\xi \rho \mathbf{L}_\xi^\dagger - \frac{1}{2} \{ \mathbf{L}_\xi^\dagger \mathbf{L}_\xi, \rho \} \right) + \eta^2 \kappa_\xi^\uparrow \left(\mathbf{L}_\xi^\dagger \rho \mathbf{L}_\xi - \frac{1}{2} \{ \mathbf{L}_\xi \mathbf{L}_\xi^\dagger, \rho \} \right), \quad (51)$$

where κ_ξ^\uparrow are the decay rates and $\mathbf{L}_\xi = \sum_{q>0} \mathbf{L}_{\xi,q}^\downarrow$. If, instead, the decay processes are local we have

$$\dot{\rho} = -i[\mathbf{H}_\xi, \rho] + \eta^2 \sum_{q>0} \sum_{\alpha=\uparrow,\downarrow} \kappa_{\xi,q}^\alpha \left(\mathbf{L}_{\xi,q}^\alpha \rho \mathbf{L}_{\xi,q}^{\alpha\dagger} - \frac{1}{2} \{ \mathbf{L}_{\xi,q}^{\alpha\dagger} \mathbf{L}_{\xi,q}^\alpha, \rho \} \right). \quad (52)$$

Then, the jump operators destroy/create a pair of fermions of momentum $\pm q$ (see App. D), i.e., $\mathbf{L}_{\xi,q}^\downarrow |m_q\rangle \propto m_q |m_q - 1\rangle$. At zero temperature, we have $\kappa_\xi^\uparrow = \kappa_{\xi,q}^\uparrow = 0$ and $\text{As}(\mathcal{H}) = \text{span}\{|p, \text{GS}\rangle \langle p', \text{GS}|\}$ for $p, p' = \pm 1$ which allows for a multistable region. In analogy to the examples of Sec. 4, it is the nature of the jump operators that discriminates the dynamics in Eq. (51) from that of Eq. (52).

5.2 The battle against decoherence

Before analyzing the stability of the open XY model as a time crystal, our aim is to identify when such a system will thermalize. We start noting that parity symmetry in the XY model gives rise to the four-dimensional asymptotic space $\text{As}(\mathcal{H}) = \text{span}\{|p, \text{GS}\rangle \langle p', \text{GS}|\}$ with $p, p' = \pm$. In the ordered phase, the dynamics described by Eq. (51) and Eq. (52), periodically concatenated with the unitary kick $\mathbf{U}_K = \mathbf{P}$, can display subharmonic oscillations. In particular, when the two ground states are perfectly degenerate, for any $\rho \in \text{As}(\mathcal{H})$ we have $\dot{\rho} = 0$, i.e., it is a steady asymptotic space. Consider the local order parameter $\mathbf{O} = \mathbf{m}_x = 1/L \sum_r \mathbf{X}_r$ and its expectation value $m_x = \langle \mathbf{m}_x \rangle$. Consider $\rho \in \text{As}(\mathcal{H})$ with entries $\rho_{pp'}$, then

$$m_x(nT) = \langle \mathbf{m}_x(nT) \rangle_\rho = \rho_{++} \langle \mathbf{m}_x \rangle_+ + \rho_{--} \langle \mathbf{m}_x \rangle_- + (-)^n (\rho_{+-} \langle +|\mathbf{m}_x| - \rangle + \text{c.c.}). \quad (53)$$

This has an important implication: the oscillations are detected only when the asymptotic state retains some coherence between parity blocks. Then, when and why will coherence be lost? Consider the vectorized space $\mathcal{H} \otimes \mathcal{H}$, and a partition between parity eigenblocks and coherences between them:

$$|\rho\rangle\rangle = \begin{pmatrix} \rho_{++} \\ \rho_c \\ \rho_{--} \end{pmatrix}, \quad \mathcal{L} = \left(\begin{array}{c|c|c} \mathcal{L}_+ & 0 & 0 \\ \hline 0 & \mathcal{L}_c & 0 \\ \hline 0 & 0 & \mathcal{L}_- \end{array} \right), \quad (54)$$

where \mathcal{L}_\pm are *bona fide* Liouvillians acting on the positive and negative parity blocks. It remains to check the action on the coherence part ρ_c . We consider the case at zero temperature, the local master equation in Eq. (51) applied to a general coherence $\rho_c = |+, \vec{m}\rangle \langle -, \vec{m}|$ (see App. D) yields

$$\partial_t |\rho_c\rangle\rangle = - \left(\sum_{q>0} \kappa_{\xi,q}^\downarrow \sin^2 \theta_{\xi,q} m_q \right) |\rho_c\rangle\rangle, \quad (55)$$

giving rise to an exponential decay of the coherence of the excited modes. Note that the coherences in the ground subspace do not decay since $m_q = 0 \forall q$. Therefore, subharmonic oscillations can be seen as long as the initial state has some coherence in $\text{As}(\mathcal{H})$. Of course, this is true assuming $\mathbf{U}_K = \mathbf{P}$. If we commit an error in the parity, the coherence in the asymptotic subspace can be mapped to coherence between some higher excited states. Then, the subsequent dissipation will decohere the state leading to a thermalized state in the (very) long time. Here is where we take advantage of the collective dissipation process. As we identified in Sec. 4, coherences can be preserved for collective decay processes. Hence, we expect the collective equation to be more robust against errors. In the following section, we analyze this possibility and compare the local and collective decay processes.

6 Characterization of the open-XY time crystal

In this section, we aim at characterizing the open-XY time crystal. We do it combining analytic and numerical tools and being primarily interested in evaluating properties (I)-(III) stated in Sec. 3. Of course, this analysis becomes costly very fast, as the number of spins L increases. Recall that the dimension of $\mathcal{L} \in \text{Op}(\mathcal{H} \otimes \mathcal{H})$ is $d_{\mathcal{H}}^2 \times d_{\mathcal{H}}^2$. Therefore, we analyze the dynamics for relative small system size and expect that the results will not depend strongly on the system size.

6.1 Time translation symmetry breaking

We start by analyzing for which parameters ξ the response of the system is subharmonic. As it is shown in Fig. 2a, the subharmonic response survives to long times when the system is kicked properly, that is, with $\mathbf{H}_K = \frac{\pi}{2} \sum_n \delta(t - nT) \mathbf{M}_z$ at any point of the phase diagram with $h < 1$. However, if the two ground-states are not exactly degenerate the oscillations may show beats. Hence, either along the factorization line (see App. C) for finite L or at any point of the ordered phase in the thermodynamic limit $L \rightarrow \infty$ subharmonic oscillations are predicted to be observed (see Fig. 2).

6.2 Coupling to higher states via an error in the parity

Time crystals are expected to have some robustness against an error in the protocol. This behavior is corresponded with condition (II) when the –small– error in the protocol is generated by a too-long $(\pi + \eta)$ -pulse. Instead of implementing the unitary rotation $\mathbf{U}_K(0) = \mathbf{P}$, the implemented unitary rotation for small η reads:

$$\mathbf{U}_K(\eta) = \left(\mathbf{1} - i \frac{\eta}{2} \mathbf{M}_z + \mathcal{O}(\eta^2) \right) \mathbf{P}. \quad (56)$$

Therefore the quantum channel $\mathcal{E}_F(\eta)$ will depend on the rotation error η . Expanding perturbatively the channel we obtain

$$\mathcal{E}_F(\eta)\rho \approx \mathcal{E}_F(0)\rho - i \frac{\eta}{2} [\mathbf{M}_z, \mathcal{E}_F(0)\rho] + \mathcal{O}(\eta^2) = (\mathcal{E}_F(0) + \eta \mathcal{V})\rho + \mathcal{O}(\eta^2), \quad (57)$$

where we have defined $\mathcal{V} = -i/2[\mathbf{M}_z, \mathcal{E}_F(0)]$. Therefore, we can get an idea of the robustness of this channel by evaluating the *distance* between the expected state after one evolution period for a perfect protocol and with an error η . As a figure of merit, we consider $1 - F(\rho(\eta, T), \rho(0, T))$, where $F(\rho, \sigma)$ is the fidelity between quantum states, which upperbounds the trace distance squared. Taking as initial state the ground state $|0, \text{GS}\rangle$ at every point of the diagram, and computing $1 - F(\rho(\eta, T), \rho(0, T))$ for $\eta = 0.05\pi$, we obtain

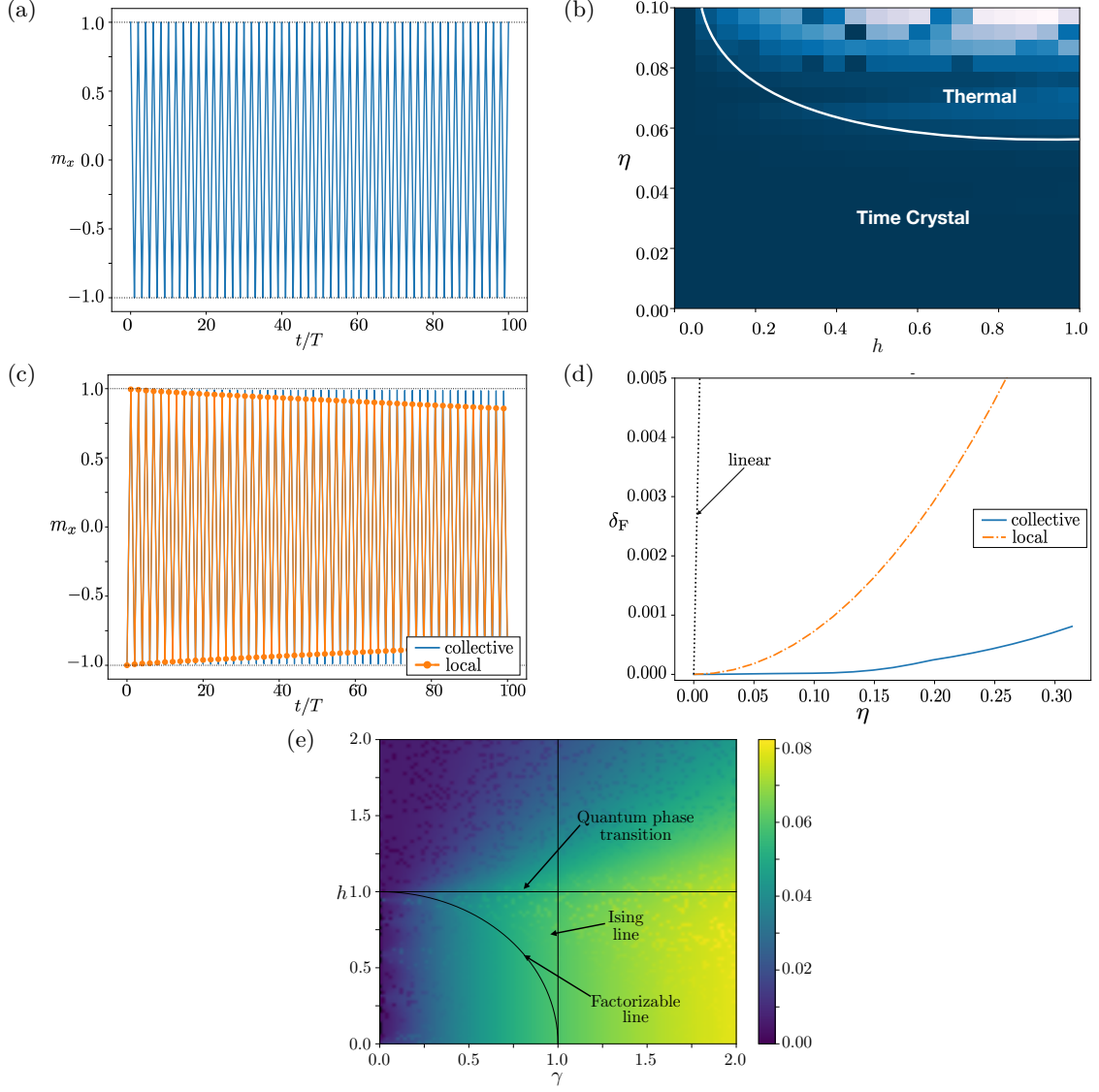


Figure 2: (a) Time translation symmetry breaking in a chain of $L = 10$ particles of the XY-open chain at the Ising point. (b) Phase diagram for the XY open chain along the factorization line with $L = 6$ and considering collective decay operators. The diagram displays two phases: Time crystal and Thermal. (c) Comparison between the dynamic evolution at the Ising point for collective (blue) and local (orange) jump operators for $L = 6$ and fixed error $\eta = 0.1$. (d) Robustness against rotation errors at the Ising point for collective (blue) and local (orange) jump operators for $L = 6$. (e) Fidelity pseudodistance between the state of the system rotated with a perfect protocol ($\eta = 0$) and the state rotated with $\eta = 0.05\pi$. Comment: The dynamics is solved with a standard fourth order Runge-Kutta. The stability is analyzed through the spectrum of the Liouvillian, obtained via exact diagonalization.

the result shown in Fig. 2e. Because the ground states are invariant under the dissipative dynamics, the only effect comes from the error in the unitary part. We see that the error is smaller closer to the isotropic line $\gamma = 0$. This can be understood easily since, for $\gamma = 0$, the system has a continuous symmetry generated by the magnetization \mathbf{M}_z . Therefore, the action of \mathcal{V} on eigenstates of the system will be negligible. On the other hand, as h grows, the ground states of the system become closer and closer to the magnetization eigenstate $|\text{GS}\rangle \approx |\uparrow\rangle^{\otimes L}$, which is invariant under any rotation generated by \mathbf{M}_z . In the rest of the parameter space, the error is approximately linear in η . Even though this seems to indicate that the time crystal is more robust around $\gamma = 0$, the most relevant feature for robustness is the collective nature of the jump operators. Hence, we show most of the results at the Ising point where the collective decay processes are encountered.

6.3 The phase diagram

The time crystal phase is often associated with a region of non-zero measure of the parameter space. In Fig. 2, we show the collective phase diagram for the open XY chain which exhibits two distinct phases of matter: a thermal phase and a time-crystal phase. The brightness of the heat map indicates the distance $\delta_F = \min_{\mu} |\varepsilon_{\mu} + 1|$, that is, the spectral distance to the ideal subharmonic state.

In the thermal phase, the error produced in the kick operation induces decoherence in the system leading to a thermalized final state. When the baths are at zero temperature, thermalization leads to the statistical mixture $\rho_{\text{th}} = 1/2(|+, \text{GS}\rangle \langle +, \text{GS}| + |-, \text{GS}\rangle \langle -, \text{GS}|)$, for which oscillations in m_x are no longer visible. Contrarily, in the time-crystal phase the collective dissipation protects the system from thermalization, leading to the observation of robust subharmonic oscillations on the order parameter m_x . Ideally, the state on the time-crystal phase is given, after n periods, by $\rho(mT) = |k \oplus m, \text{GS}\rangle \langle k \oplus m, \text{GS}|$ with $k = 0, 1$.

6.4 Preserving coherence for a Long-time TC

As we have briefly discussed in Sec. 5, the main process for which the oscillations in the time-crystal may die out is decoherence. We also have discussed in Sec. 4 that collective jump operators preserve coherence during the evolution. Hence, it is interesting to compare the robustness of collective and local master equations. In panel (c) of Fig. 2, we compare the dynamics evolution of the collective (blue) and local (orange) master equations for a system of $L = 6$ spins when an error $\eta = 0.1$ is committed during the rotation. As discussed previously, the oscillations are robust when the dissipation is generated by collective jump operators while it clearly decays when the jump operators are local.

In panel (d) we show the scaling with η of the distance $\delta_F = \min_{\mu} |\varepsilon_{\mu} + 1|$ for collective (blue) and local (orange) decay processes. The derivative of this plot at $\eta = 0$ corresponds to the susceptibility $\chi^{(1)}$.

7 Conclusions

In this article we have presented some self-contained results concerning the existence and properties of time crystals in open systems whose evolution is described with a Lindblad master equation. After introducing the tools of Markovian quantum open system dynamics, we have provided a compact definition of an open system time crystal derived from the properties the spectrum of the Floquet propagator. We have, as well, identified which are the most relevant properties of this object with special emphasis on the relevant aspects

of the asymptotic subspace structure and the conserved quantities. We have analytically solved the kicked dynamics of an exemplary set of one and two-qubit open system models and exploit such analysis to provide key features on the properties and stability of time crystals in open systems. Finally, we have derived and analyzed the open XY model as a time-crystal. There has been some discussion around the possibility that only *long-range* models can exhibit time-crystalline order in open quantum systems, our analysis shows that this is not the case and we conclude that long-range interactions are not crucial features to observe time-crystalline behavior. Nonetheless, our findings show that *long-range* (or collective) jump operators are crucial in order to have subharmonic oscillations that are more robust to rotation errors. Intuitively, the collective jump operators help to preserve coherence in the dissipation process, and the time-crystalline oscillations are usually coherent in the Hamiltonian eigenbasis. Moreover, at the time of completion of this manuscript, it was noted in [43] that permutationally invariant systems are, also, robust to disorder. In App. F we show that the same idea apply to the open XY time-crystal presented in this work.

To conclude, in agreement with [26], we believe that a promising direction of investigation is that of non-Markovian environments. There, the backflow of information to the system may be controlled to achieve subharmonic response.

A Mathematical properties of \mathcal{L}

For completeness, we include here some discussion about the mathematical properties outlined in Sec. 2 of the main text.

If a particular eigenvalue λ_μ of \mathcal{L} has algebraic multiplicity $m_\mu \geq 1$, the number of non-trivial solutions of Eq. (6) lies between one and m_μ . If there is strictly one solution $|\mathbf{r}_\mu\rangle\rangle$ associated to λ_μ but $m_\mu > 1$, higher rank generalized eigenvalues can be found as solutions of the recursive equation $(\mathcal{L} - \lambda_\mu \mathcal{I})|\mathbf{r}_\mu(s)\rangle\rangle = |\mathbf{r}_\mu(s-1)\rangle\rangle$, where $|\mathbf{r}_\mu(1)\rangle\rangle = |\mathbf{r}_\mu\rangle\rangle$ and s denotes the rank. Note that $(\mathcal{L} - \lambda_\mu \mathcal{I})^k |\mathbf{r}_\mu(s)\rangle\rangle = 0$ only if $k \geq s$.

(i) Spectrum of the Liouvillian:

Consider $\mathbf{r}_\mu \in \text{Op}(\mathcal{H})$ such that $\mathcal{L}\mathbf{r}_\mu = \lambda_\mu \mathbf{r}_\mu$. Then, hermiticity preservation $\mathcal{L}\mathbf{r}_\mu^\dagger = (\mathcal{L}\mathbf{r}_\mu)^\dagger$ guarantees

$$\mathcal{L}\mathbf{r}_\mu^\dagger = (\mathcal{L}\mathbf{r}_\mu)^\dagger = \lambda_\mu^* \mathbf{r}_\mu^\dagger, \quad (58)$$

that is, either the eigenvalues are real or come by conjugate pairs. Note that if $\mathbf{r}_\mu = \mathbf{r}_\mu^\dagger$ $\lambda_\mu \in \mathbb{R}$. The converse is true, at least, when λ_μ is non-degenerate.

(ii.1) Eigenvectors of different eigenvalue are linearly independent:

Consider the linear combination $\sum_\mu c_\mu |\mathbf{r}_\mu\rangle\rangle = 0$, where $|\mathbf{r}_\mu\rangle\rangle$ are eigenvectors of different eigenvalue of \mathcal{L} . If one multiplies the linear combination by the operator $\prod_{\nu \neq \mu} (\mathcal{L} - \lambda_\nu \mathcal{I})$ it leads to $c_\mu \mathbf{r}_\mu = 0$, and therefore the set $\{|\mathbf{r}_\mu\rangle\rangle\}_\mu$ is linearly independent by definition.

(ii.2) Generalized eigenvectors are linearly independent:

Consider the simplified case where there is only one eigenvector $|\mathbf{r}_\mu(0)\rangle\rangle$ for the eigenvalue λ_μ . Consider the linear combination $\sum_k c_k |\mathbf{r}_\mu(k)\rangle\rangle = 0$. Then, by successive applications of the operator $\mathcal{L} - \lambda_\mu \mathcal{I}$ we obtain $c_k = 0 \forall k$ and then the set $\{|\mathbf{r}_\mu(k)\rangle\rangle\}_k$ is linearly independent.

This prove can be extended using similar methods to the complete set of generalized eigenvectors $\{|\mathbf{r}_\mu(k)\rangle\rangle\}_{\mu,k}$ of \mathcal{L} . Then, the complete set of generalized eigenvectors forms a basis of the space.

(iii.1) Biorthogonality of left and right eigenvectors:

Consider $\{|\mathbf{l}_\mu(k)\rangle\rangle\}_{\mu,k}$ and $\{|\mathbf{r}_\mu(k)\rangle\rangle\}_{\mu,k}$ the set of left and right generalized eigenvectors. Then,

$$\langle\langle \mathbf{l}_\mu(1) | (\mathcal{L} - \lambda_\nu \mathcal{I}) | \mathbf{r}_\nu(1) \rangle\rangle = 0 \Rightarrow (\lambda_\mu - \lambda_\nu) \langle\langle \mathbf{l}_\mu(1) | \mathbf{r}_\nu(1) \rangle\rangle = 0, \quad (59)$$

and, therefore, eigenvectors of different eigenvalues can be chosen biorthonormal. For a diagonalizable matrix, the biorthogonal relation can be compactly written as $\mathcal{W}_l^\dagger \mathcal{W}_r = \mathcal{I}$.

(iii.2) Normal Jordan form:

Given \mathcal{L} , it exists a similarity transformation \mathcal{W}_r such that $\mathcal{W}_r^{-1} \mathcal{L} \mathcal{W}_r = \mathcal{J}$ where \mathcal{J} is in Jordan canonical form such that the columns \mathcal{W}_r are the generalized eigenvectors $|\mathbf{r}_\mu(s)\rangle\rangle$. This corresponds to solving the generalized eigenvalue equation $\mathcal{L} \mathcal{W}_r = \mathcal{W}_r \mathcal{J}$.

(iv) Time-ordered propagator:

This is the well-known solution of a linear equation with time-dependent coefficients when the generator may not commute with itself at different times.

(v.1) **Existence of the steady-state:**

The trace preserving condition for an arbitrary state ρ , together with Eq. (5) lead to:

$$\text{tr}[\mathcal{L}\rho] = \text{tr}[(\mathcal{L}^\dagger \mathbf{1})^\dagger \rho] = 0, \quad (60)$$

guarantees at least one eigenvalue $\lambda_0 = 0$. The corresponding eigenvector $\rho_\infty = \mathbf{r}_0$ fulfills that $\partial_t \rho_\infty = 0$, and it is often referred to the steady-state. In general, however, the steady-state may not be unique.

(v.2) **Contractivity of the evolution. Convergence to $\text{As}(\mathcal{H})$:**

We include it here the proof given in [41]. Given an Hermitian operator $\mathbf{O} = \mathbf{O}_+ - \mathbf{O}_-$ where \mathbf{O}_\pm are positive matrices, and a CPTP map \mathcal{E} , it follows that

$$\text{tr}|\mathcal{E}\mathbf{O}| = \text{tr}|\mathcal{E}\mathbf{O}_+ - \mathcal{E}\mathbf{O}_-| \leq \text{tr}|\mathcal{E}\mathbf{O}_+| + \text{tr}|\mathcal{E}\mathbf{O}_-| = \text{tr}|\mathbf{O}_+| + \text{tr}|\mathbf{O}_-| = \text{tr}|\mathbf{O}|. \quad (61)$$

In particular, given $\rho, \sigma \in \mathcal{S}(\mathcal{H})$ we see that the trace distance $D(\mathcal{E}\rho, \mathcal{E}\sigma) \leq D(\rho, \sigma)$, which provides a convergence towards the asymptotic subspace.

B Generalized susceptibilities and higher order robustness

In the main text we considered the linear susceptibility $\chi^{(1)}$. However, higher order measures of robustness can be obtained as we show this in this section. Consider a general quantum map $\mathcal{E} = \mathcal{E}_0 + \eta\mathcal{E}_1$ with $\eta \ll 1$. We aim at finding its spectrum defined via the equations:

$$\begin{aligned} \langle\langle \mathbf{1} | \mathcal{E} = \langle\langle \mathbf{1} | \varepsilon, \\ \mathcal{E} | \mathbf{r} \rangle\rangle = \varepsilon | \mathbf{r} \rangle\rangle, \end{aligned} \quad (62)$$

for a particular eigenvalue ε . We assume that \mathbf{r} , $\mathbf{1}$ and ε can be expanded in powers of η

$$\begin{aligned} | \mathbf{r} \rangle\rangle &= \sum_{k \geq 0} \eta^k | \mathbf{r}_k \rangle\rangle, \\ \langle\langle \mathbf{1} | &= \sum_{k \geq 0} \eta^k \langle\langle \mathbf{1}_k |, \\ \varepsilon &= \sum_{k \geq 0} \eta^k \varepsilon_k. \end{aligned} \quad (63)$$

It follows that Eq. (62) can be written

$$\mathcal{E}_0 | \mathbf{r}_0 \rangle\rangle + \sum_{k \geq 1} \eta^k (\mathcal{E}_0 | \mathbf{r}_k \rangle\rangle + \mathcal{E}_1 | \mathbf{r}_{k-1} \rangle\rangle) = \sum_{k \geq 1} \sum_{l=1}^k \eta^k \varepsilon_l | \mathbf{r}_{k-l} \rangle\rangle + \sum_{k \geq 0} \eta_k \varepsilon_0 | \mathbf{r}_k \rangle\rangle, \quad (64)$$

which leads to the recurrence relation:

$$(\mathcal{E}_0 - \lambda_0) | \mathbf{r}_k \rangle\rangle = \mathcal{E}_1 | \mathbf{r}_{k-1} \rangle\rangle - \sum_{l=1}^k \varepsilon_l | \mathbf{r}_{k-l} \rangle\rangle. \quad (65)$$

The correction to the eigenvalues can be computed by projecting onto $\langle\langle \mathbf{l}_0 |$,

$$\varepsilon_k = \langle\langle \mathbf{l}_0 | \mathcal{E}_1 | \mathbf{r}_{k-1} \rangle\rangle - \sum_{l=1}^{k-1} \varepsilon_l \langle\langle \mathbf{l}_0 | \mathbf{r}_{k-l} \rangle\rangle, \quad (66)$$

with the relation

$$\varepsilon_k = \frac{1}{k!} \left. \frac{\partial^k \varepsilon}{\partial^k \eta} \right|_{\eta=0}. \quad (67)$$

Perturbed eigenvectors can be also computed from Eq. (65), however its expression is quite involved and dependent on the choice of the inverse of the operator $\mathcal{E}_0 - \lambda_0$ [42] and we do not include them here.

C XY chain: A sub-manifold of product ground states

There exists a particular sub-manifold ξ_p of the parameter space ξ (within the ordered phase $h < 1$) such that the ground space of the system can be analytically found as product of rotated spin states. This manifold is often referred as the factorization line. This sub-manifold is described by the radius-one circle $h^2 + \gamma^2 = 1$, or equivalently, $\xi_p = (J, \sqrt{1 - h^2}, h)$ [37]. The exactly degenerated ground states are found:

$$|k, \text{GS}\rangle = \prod_{r=1}^L \left(\cos \zeta |\uparrow\rangle_r + (-)^k \sin \zeta |\downarrow\rangle_r \right) \quad \text{for } k = 0, 1, \quad (68)$$

where $\cos^2(2\zeta) = (1 - \gamma)/(1 + \gamma)$. Note that this includes the Ising Hamiltonian at zero transverse field. Also, both states are connected via $\mathbf{P} |k, \text{GS}\rangle = |k \oplus 1, \text{GS}\rangle$ where \oplus means sum modulo two. This allows to define a ground state within each parity sector as

$$|p, \text{GS}\rangle = \frac{|0, \text{GS}\rangle + p |1, \text{GS}\rangle}{\sqrt{2}}, \quad (69)$$

such that $\mathbf{P} |p, \text{GS}\rangle = p |p, \text{GS}\rangle$. The associated dispersion relation is for each of these ground states is:

$$\omega_{\lambda, q} = J \left| 1 - h \cos \left(\frac{2\pi}{L} q \right) \right|. \quad (70)$$

D XY chain: Pseudo-spin representation

We start by rewriting the Hamiltonian of the system summed over only the positive quasi-momentum part. From Eq. (46), we find

$$\begin{aligned} \mathbf{H}_\xi^\pm &= \sum_{q>0} \omega_{\xi, q} \left(\mathbf{d}_{\xi, q}^\dagger \mathbf{d}_{\xi, q} - \mathbf{d}_{\xi, -q}^\dagger \mathbf{d}_{\xi, -q} \right) + \\ &+ \frac{(1 \mp 1)}{2} \left(\omega_{\xi, 0} (\mathbf{d}_0 \mathbf{d}_0^\dagger - \mathbf{d}_0^\dagger \mathbf{d}_0) + \omega_{\xi, \pi} (\mathbf{d}_\pi \mathbf{d}_\pi^\dagger - \mathbf{d}_\pi^\dagger \mathbf{d}_\pi) \right) \end{aligned} \quad (71)$$

where $q > 0 = \{1/2, \dots, (L-1)/2\}$, a total of $L/2$ values; and $q > 0 = \{1, \dots, L/2 - 1\}$, a total of $L/2 - 1$ values, for the even and odd parity sectors respectively. Folding the BZ into the $q > 0$ part, the full Fock space for a given quasimomentum q is spanned by

the four states $|0\rangle_q$, $\mathbf{c}_q^\dagger|0\rangle_q$, $\mathbf{c}_{-q}^\dagger|0\rangle_q$, and $\mathbf{c}_q^\dagger\mathbf{c}_{-q}^\dagger|0\rangle_q$. Within the vanishing *total* quasi-momentum subspace, defined by $\mathbf{Q} = \sum_q q\mathbf{d}_q^\dagger\mathbf{d}_q$, the states can be labeled with binary numbers collected in the vector \vec{m} , such that

$$|\pm, \vec{m}\rangle = \begin{cases} \prod_{q>0} (\mathbf{c}_q^\dagger\mathbf{c}_{-q}^\dagger)^{m_k} |+, \text{vac}\rangle \\ \mathbf{c}_0^\dagger \prod_{q>0} (\mathbf{c}_q^\dagger\mathbf{c}_{-q}^\dagger)^{m_k} |-, \text{vac}\rangle, \end{cases} \quad (72)$$

with the subtlety that the $q = -\pi$ mode should be unoccupied for the odd parity sector when L is even. This comes from the fact that the mode $-q = q = -\pi$ goes into itself at the borders of the Brillouin zone. If the system is prepared in a state of the subspace of vanishing *total* quasi-momentum q , for instance $|\pm, \text{GS}\rangle$, a pseudo-spin representation is possible for each block q . This is because \mathbf{H}_ξ^\pm only connects the Fock vacuum (of the physical fermions) $|\text{vac}\rangle$ with the state $\mathbf{c}_q^\dagger\mathbf{c}_{-q}^\dagger|\text{vac}\rangle$ for each q . We introduce the notation:

$$\mathbf{c}_q^\dagger\mathbf{c}_{-q}^\dagger|\text{vac}\rangle_q \leftrightarrow |\uparrow\rangle_q \quad \& \quad |\text{vac}\rangle_q \leftrightarrow |\downarrow\rangle_q. \quad (73)$$

Then for any operator $\mathbf{O} = \sum_q \mathbf{O}_q$, that acts independently on the different subspaces of quasi-momentum q , we can decompose it in this basis as:

$$\mathbf{O}_q = \sum_{ss'=\uparrow\downarrow} \langle s|\mathbf{O}_q|s'\rangle |s\rangle\langle s'|. \quad (74)$$

In the second-quantization, the expression of \mathbf{O} is given by:

$$\mathbf{O} = \sum_{q>0} \begin{pmatrix} \mathbf{c}_q^\dagger & \mathbf{c}_{-q} \end{pmatrix} \begin{pmatrix} O_{q,\uparrow\uparrow} & O_{q,\uparrow\downarrow} \\ O_{q,\downarrow\uparrow} & O_{q,\downarrow\downarrow} \end{pmatrix} \begin{pmatrix} \mathbf{c}_q \\ \mathbf{c}_{-q}^\dagger \end{pmatrix}. \quad (75)$$

E Detailed derivation of the Master Equation

Our starting point is the system-bath Hamiltonian in Eq. (38). For simplicity of the calculation, we also restrict ourselves to the zero quasi-momentum subspace. For further use, we introduce the interaction picture as $\mathbf{O}(t) = \exp(i\mathbf{H}_S t)\mathbf{O}\exp(-i\mathbf{H}_S t)$. Our starting point is the Redfield equation in the interaction picture:

$$\dot{\tilde{\rho}}(t) = -\text{tr}_B \int_0^\infty ds [\mathbf{H}_{\text{SB}}(t), [\mathbf{H}_{\text{SB}}(t-s), \tilde{\rho}(t) \otimes \rho_{\text{eq}}]], \quad (76)$$

where $[\rho_{\text{eq}}, \mathbf{H}_B] = 0$. Next, we decompose the magnetization operator according to:

$$\begin{aligned} \mathbf{M}_z &= \sum_r (1 - 2\mathbf{c}_r^\dagger\mathbf{c}_r) = \sum_q (1 - 2\mathbf{c}_q^\dagger\mathbf{c}_q) = -2 \sum_{q>0} (\mathbf{c}_q^\dagger\mathbf{c}_q - \mathbf{c}_{-q}\mathbf{c}_{-q}^\dagger) \\ &= -2 \sum_{q>0} \begin{pmatrix} \mathbf{d}_q^\dagger & \mathbf{d}_{-q} \end{pmatrix} \begin{pmatrix} \cos(\theta_{\xi,q}) & \sin(\theta_{\xi,q}) \\ \sin(\theta_{\xi,q}) & -\cos(\theta_{\xi,q}) \end{pmatrix} \begin{pmatrix} \mathbf{d}_q \\ \mathbf{d}_{-q}^\dagger \end{pmatrix}. \end{aligned} \quad (77)$$

Note that this gives rise to the partition introduced in Eq. (49) of the main text in terms of the jump operators $\mathbf{L}_{\xi,q}^\alpha$. Introducing this partition in Eq. (76) it follows

$$\dot{\tilde{\rho}}(t) = \eta^2 \sum_{q,q'>0} \sum_{\alpha,\alpha'} \int_0^\infty ds \left(\mathbf{L}_{\xi,q'}^\alpha(t-s)\tilde{\rho}(t)\mathbf{L}_{\xi,q}^{\alpha\dagger}(t) - \mathbf{L}_{\xi,q}^{\alpha\dagger}(t)\mathbf{L}_{\xi,q'}^\alpha(t-s)\tilde{\rho}(t) \right) C(s) + \text{h.c.}, \quad (78)$$

where $C(t-t') = \text{tr}_B[\mathbf{B}(t)\mathbf{B}(t')\rho_{\text{eq}}]$. Note that, by construction $\mathbf{L}_{\xi,q}^\alpha(t) = \mathbf{L}_{\xi,q}^\alpha(0) \exp(iE_{\xi,q}^\alpha t)$ and $E_{\xi,q}^0 = 0$, $E_{\xi,q}^\dagger = \pm 2\omega_{\xi,q}$ and then

$$\dot{\tilde{\rho}}(t) = -\eta^2 \sum_{q,q'>0} \sum_{\alpha,\alpha'} \Gamma(E_{\xi,q}^\alpha) e^{-i(E_{\xi,q}^\alpha - E_{\xi,q'}^{\alpha'})t} \left(\mathbf{L}_{\xi,q}^{\alpha\dagger} \mathbf{L}_{\xi,q'}^{\alpha'} \tilde{\rho}(t) - \mathbf{L}_{\xi,q'}^{\alpha'} \tilde{\rho}(t) \mathbf{L}_{\xi,q}^{\alpha\dagger} \right) + \text{h.c.} \quad (79)$$

where we have introduced $\Gamma(\omega) = \int_0^\infty ds C(s) \exp(i\omega s)$. We take the real and imaginary parts of $\Gamma(\omega)$ as follows:

$$\begin{aligned} \Gamma(\omega) &= \frac{1}{2} \kappa(\omega) + iS(\omega), \\ \kappa(\omega) &= \int_0^\infty ds C(s) e^{i\omega s} + \int_0^\infty C^*(s) e^{-i\omega s} = \int_{-\infty}^\infty ds C(s) e^{i\omega s} = C(\omega), \\ S(\omega) &= \frac{1}{2i} \left(\int_0^\infty ds C(s) e^{i\omega s} - \int_0^\infty ds C^*(s) e^{i\omega s} \right). \end{aligned} \quad (80)$$

Then, we can compute the bath correlation function as:

$$\begin{aligned} C(s) &= \sum_{kk',\mu\mu'} \left\langle \left(g_{k,\mu} \mathbf{b}_{k,\mu}^\dagger e^{i\omega_{k,\mu}s} + g_{k',\mu}^* \mathbf{b}_{k,\mu} e^{-i\omega_{k,\mu}s} \right) \left(g_{k',\mu'} \mathbf{b}_{k',\mu'}^\dagger + g_{k',\mu'}^* \mathbf{b}_{\alpha',\mu'} \right) \rho_{\text{eq}} \right\rangle \\ &= \sum_{k,\mu} |g_{k,\mu}|^2 \left(n_k(\omega_{k,\mu}) e^{i\omega_{k,\mu}s} + (1 + n_k(\omega_{k,\mu})) e^{-i\omega_{k,\mu}s} \right) \\ &= \sum_k \int_0^\infty \frac{d\omega}{2\pi} J_k(\omega) \left(n_k(\omega) e^{i\omega s} + (1 + n_k(\omega)) e^{-i\omega s} \right), \end{aligned} \quad (81)$$

where we have introduced the spectral density $J_k(\omega) = 2\pi \sum_\mu |g_{k,\mu}|^2 \delta(\omega - \omega_{k,\mu})$. When the number of the modes of the bath tends to infinity, the spectral function is usually approximated with a continuous function of ω . The spectral function $J_k(\omega)$ can be analytically continued towards negative frequencies as $J_k(-\omega) = -J_k(\omega)$, which allows:

$$C(s) = \sum_k \int_{-\infty}^\infty \frac{d\omega}{2\pi} J_k(\omega) (1 + n_k(\omega)) e^{-i\omega s}, \quad (82)$$

and reading of $C(\omega) = \sum_k J_k(\omega) (1 + n_k(\omega))$. The function $S(\omega)$ is given

$$S(\omega) = \text{Im} \left[\sum_k \int_{\mathbb{R}} \frac{d\omega'}{2\pi} J_k(\omega') (n_k(\omega') + 1) \int_0^\infty ds e^{i(\omega - \omega')s} \right] = \sum_k \mathcal{P} \int_{\mathbb{R}} \frac{d\omega'}{2\pi} \frac{J_k(\omega') (n_k(\omega') + 1)}{\omega - \omega'}, \quad (83)$$

and it is responsible for the Lamb shift. From now on, it will be ignored which corresponds to substituting $\Gamma(\omega) \rightarrow 1/2\kappa(\omega)$ in Eq. (79). Note that, since $\kappa(\omega = 0) = 0$, the jump operators $\mathbf{L}_{\xi,q}^0$ will not contribute to dissipation at zero temperature. For finite temperature, they will not contribute either if the spectral density is super-ohmic, which we assume to be the case.

$$\dot{\tilde{\rho}}(t) = -\frac{\eta^2}{2} \sum_{q,q'>0} \sum_{\alpha,\alpha' \neq 0} \kappa(E_{\xi,q}^\alpha) e^{-i(E_{\xi,q}^\alpha - E_{\xi,q'}^{\alpha'})t} \left(\mathbf{L}_{\xi,q}^{\alpha\dagger} \mathbf{L}_{\xi,q'}^{\alpha'} \tilde{\rho}(t) - \mathbf{L}_{\xi,q'}^{\alpha'} \tilde{\rho}(t) \mathbf{L}_{\xi,q}^{\alpha\dagger} \right) + \text{h.c.} \quad (84)$$

The next step consists in using the secular approximation, that selects only those terms that fulfill the resonant condition $E_{\xi,q}^\alpha - E_{\xi,q'}^{\alpha'} = 0$. As explained in the main text, two

different situations can arise. We first assume that the dispersion $\omega_{\xi,q}$ is such that the transition energies are well separated, and then, resonances are individually hit for each q . Going back to the Schrödinger picture, it yields the local master equation:

$$\dot{\rho} = -i[\mathbf{H}_{\xi}, \rho] + \eta^2 \sum_{q>0} \sum_{\alpha=\uparrow,\downarrow} \kappa_{\xi,q}^{\alpha} \left(\mathbf{L}_{\xi,q}^{\alpha} \rho \mathbf{L}_{\xi,q}^{\alpha\dagger} - \frac{1}{2} \{ \mathbf{L}_{\xi,q}^{\alpha\dagger} \mathbf{L}_{\xi,q}^{\alpha}, \rho \} \right). \quad (85)$$

where $\kappa_{\xi,q}^{\downarrow} = \sum_k J_{\alpha}(2\omega_{\xi,q})(n_k(2\omega_{\xi,q}) + 1)$, and $\kappa_{\xi,q}^{\uparrow} = \sum_k J_k(2\omega_{\xi,q})n_{\alpha}(2\omega_{\xi,q})$.

If instead, the dispersion $\omega_{\xi,q} \approx \omega_0$ is approximately flat, e.g. at the Ising point with zero transverse field, then all resonances will be hit collectively and we will be able to resume the jump operators $\mathbf{L}_{\xi} = \sum_{q>0} \mathbf{L}_{\xi,q}^{\downarrow}$. This gives rise to the collective master equation:

$$\dot{\rho} = -i[\mathbf{H}_{\xi}, \rho] + \eta^2 \kappa_{\xi}^{\downarrow} \left(\mathbf{L}_{\xi} \rho \mathbf{L}_{\xi}^{\dagger} - \frac{1}{2} \{ \mathbf{L}_{\xi}^{\dagger} \mathbf{L}_{\xi}, \rho \} \right) + \eta^2 \kappa_{\xi}^{\uparrow} \left(\mathbf{L}_{\xi}^{\dagger} \rho \mathbf{L}_{\xi} - \frac{1}{2} \{ \mathbf{L}_{\xi} \mathbf{L}_{\xi}^{\dagger}, \rho \} \right), \quad (86)$$

where $\kappa_{\xi}^{\downarrow} = \sum_k J_{\alpha}(2\omega_0)(n_k(2\omega_0) + 1)$, and $\kappa_{\xi}^{\uparrow} = \sum_k J_k(2\omega_0)n_{\alpha}(2\omega_0)$.

F Robustness to disorder

At the time of completion of this manuscript it was noted in [43] that a permutationally invariant system is, to first order, robust to disorder. A similar idea can apply to the open-XY time crystal. To be more precise, consider that we kick the system with the disordered pulse

$$\mathbf{H}_K = \sum_n \delta(t - nT) \sum_{r=1}^L (\pi + \eta \delta_r) \frac{\mathbf{Z}_r}{2}, \quad (87)$$

where η parametrizes the disorder strength, δ_r is a measure of the fluctuation at site r subject to $\sum_r \delta_r = 0$. To first order in η , the evolution over one period is given by:

$$\mathcal{E}_F(\eta)\rho \approx \mathcal{E}_F(0)\rho - i\frac{\eta}{2} \sum_r \delta_r [\mathbf{Z}_r, \mathcal{E}_F(0)\rho] + \mathcal{O}(\eta^2). \quad (88)$$

Hence, the first order susceptibility $\chi^{(1)}$ can be computed as

$$\chi_{\mu}^{(1)} = \frac{|\varepsilon_{\mu}|}{2} |\langle \mathbf{1}_{\mu} | \mathbf{Z}_1 \otimes \mathbf{1} - \mathbf{1} \otimes \mathbf{Z}_1 | \mathbf{r}_{\mu} \rangle| \left(\sum_r \delta_r \right) = 0 \quad (89)$$

where we have used the permutationally invariance of the system. Therefore, it is guaranteed that the system is linearly robust to disorder.

References

- [1] Ronnie Kosloff. Quantum thermodynamics: A dynamical viewpoint. *Entropy*, 15(6): 2100–2128, 2013.
- [2] Robert Alicki and David Gelbwaser-Klimovsky. Non-equilibrium quantum heat machines. *New Journal of Physics*, 17(11):115012, 2015.
- [3] Sebastian Restrepo, Javier Cerrillo, Philipp Strasberg, and Gernot Schaller. From quantum heat engines to laser cooling: Floquet theory beyond the born–markov approximation. *New Journal of Physics*, 20(5):053063, 2018.

- [4] Wolfgang Niedenzu and Gershon Kurizki. Cooperative many-body enhancement of quantum thermal machine power. *New Journal of Physics*, 20(11):113038, 2018.
- [5] Andreu Riera-Campenya, Mohammad Mehboudi, Marisa Pons, and Anna Sanpera. Dynamically induced heat rectification in quantum systems. *Physical Review E*, 99(3):032126, 2019.
- [6] Marin Bukov, Luca D’Alessio, and Anatoli Polkovnikov. Universal high-frequency behavior of periodically driven systems: from dynamical stabilization to floquet engineering. *Advances in Physics*, 64(2):139–226, 2015.
- [7] Jérôme Cayssol, Balázs Dóra, Ferenc Simon, and Roderich Moessner. Floquet topological insulators. *physica status solidi (RRL)–Rapid Research Letters*, 7(1-2):101–108, 2013.
- [8] Adolfo del Campo. Shortcuts to adiabaticity by counterdiabatic driving. *Physical review letters*, 111(10):100502, 2013.
- [9] C. W. von Keyserlingk, Vedika Khemani, and S. L. Sondhi. Absolute stability and spatiotemporal long-range order in Floquet systems. *Phys. Rev. B*, 94:085112, Aug 2016. DOI: [10.1103/PhysRevB.94.085112](https://doi.org/10.1103/PhysRevB.94.085112). URL <https://link.aps.org/doi/10.1103/PhysRevB.94.085112>.
- [10] Vedika Khemani, C. W. von Keyserlingk, and S. L. Sondhi. Defining time crystals via representation theory. *Phys. Rev. B*, 96:115127, Sep 2017. DOI: [10.1103/PhysRevB.96.115127](https://doi.org/10.1103/PhysRevB.96.115127). URL <https://link.aps.org/doi/10.1103/PhysRevB.96.115127>.
- [11] Dominic V. Else, Bela Bauer, and Chetan Nayak. Floquet time crystals. *Phys. Rev. Lett.*, 117:090402, Aug 2016. DOI: [10.1103/PhysRevLett.117.090402](https://doi.org/10.1103/PhysRevLett.117.090402). URL <https://link.aps.org/doi/10.1103/PhysRevLett.117.090402>.
- [12] Dominic V. Else, Bela Bauer, and Chetan Nayak. Prethermal phases of matter protected by time-translation symmetry. *Phys. Rev. X*, 7:011026, Mar 2017. DOI: [10.1103/PhysRevX.7.011026](https://doi.org/10.1103/PhysRevX.7.011026). URL <https://link.aps.org/doi/10.1103/PhysRevX.7.011026>.
- [13] J Zhang, PW Hess, A Kyprianidis, P Becker, A Lee, J Smith, G Pagano, I-D Potirniche, Andrew C Potter, A Vishwanath, et al. Observation of a discrete time crystal. *Nature*, 543(7644):217, 2017.
- [14] Soonwon Choi, Joonhee Choi, Renate Landig, Georg Kucsko, Hengyun Zhou, Junichi Isoya, Fedor Jelezko, Shinobu Onoda, Hitoshi Sumiya, Vedika Khemani, et al. Observation of discrete time-crystalline order in a disordered dipolar many-body system. *Nature*, 543(7644):221, 2017.
- [15] Wen Wei Ho, Soonwon Choi, Mikhail D. Lukin, and Dmitry A. Abanin. Critical time crystals in dipolar systems. *Phys. Rev. Lett.*, 119:010602, Jul 2017. DOI: [10.1103/PhysRevLett.119.010602](https://doi.org/10.1103/PhysRevLett.119.010602). URL <https://link.aps.org/doi/10.1103/PhysRevLett.119.010602>.
- [16] N. Y. Yao, A. C. Potter, I.-D. Potirniche, and A. Vishwanath. Discrete time crystals: Rigidity, criticality, and realizations. *Phys. Rev. Lett.*, 118:030401, Jan 2017. DOI: [10.1103/PhysRevLett.118.030401](https://doi.org/10.1103/PhysRevLett.118.030401). URL <https://link.aps.org/doi/10.1103/PhysRevLett.118.030401>.
- [17] Zongping Gong, Ryusuke Hamazaki, and Masahito Ueda. Discrete time-crystalline order in cavity and circuit qed systems. *Physical review letters*, 120(4):040404, 2018.
- [18] F. Iemini, A. Russomanno, J. Keeling, M. Schirò, M. Dalmonte, and R. Fazio. Boundary time crystals. *Phys. Rev. Lett.*, 121:035301, Jul 2018. DOI: [10.1103/PhysRevLett.121.035301](https://doi.org/10.1103/PhysRevLett.121.035301). URL <https://link.aps.org/doi/10.1103/PhysRevLett.121.035301>.

- [19] Frank Wilczek. Quantum time crystals. *Phys. Rev. Lett.*, 109:160401, Oct 2012. DOI: [10.1103/PhysRevLett.109.160401](https://doi.org/10.1103/PhysRevLett.109.160401). URL <https://link.aps.org/doi/10.1103/PhysRevLett.109.160401>.
- [20] Patrick Bruno. Impossibility of spontaneously rotating time crystals: A no-go theorem. *Phys. Rev. Lett.*, 111:070402, Aug 2013. DOI: [10.1103/PhysRevLett.111.070402](https://doi.org/10.1103/PhysRevLett.111.070402). URL <https://link.aps.org/doi/10.1103/PhysRevLett.111.070402>.
- [21] Angelo Russomanno, Fernando Iemini, Marcello Dalmonte, and Rosario Fazio. Floquet time crystal in the lipkin-meshkov-glick model. *Phys. Rev. B*, 95:214307, Jun 2017. DOI: [10.1103/PhysRevB.95.214307](https://doi.org/10.1103/PhysRevB.95.214307). URL <https://link.aps.org/doi/10.1103/PhysRevB.95.214307>.
- [22] Biao Huang, Ying-Hai Wu, and W. Vincent Liu. Clean floquet time crystals: Models and realizations in cold atoms. *Phys. Rev. Lett.*, 120:110603, Mar 2018. DOI: [10.1103/PhysRevLett.120.110603](https://doi.org/10.1103/PhysRevLett.120.110603). URL <https://link.aps.org/doi/10.1103/PhysRevLett.120.110603>.
- [23] Achilleas Lazarides and Roderich Moessner. Fate of a discrete time crystal in an open system. *Physical Review B*, 95(19):195135, 2017.
- [24] F. M. Gambetta, F. Carollo, M. Marcuzzi, J. P. Garrahan, and I. Lesanovsky. Discrete time crystals in the absence of manifest symmetries or disorder in open quantum systems. *Phys. Rev. Lett.*, 122:015701, Jan 2019. DOI: [10.1103/PhysRevLett.122.015701](https://doi.org/10.1103/PhysRevLett.122.015701). URL <https://link.aps.org/doi/10.1103/PhysRevLett.122.015701>.
- [25] Bihui Zhu, Jamir Marino, Norman Yao, Mikhail D Lukin, and Eugene Demler. Dicke time crystals in driven-dissipative quantum many-body systems. *New Journal of Physics*, 2019.
- [26] Achilleas Lazarides, Sthitadhi Roy, Francesco Piazza, and Roderich Moessner. On time crystallinity in dissipative Floquet systems. *arXiv preprint arXiv:1904.04820*, 2019.
- [27] Heinz-Peter Breuer, Francesco Petruccione, et al. *The theory of open quantum systems*. Oxford University Press on Demand, 2002.
- [28] Robert Alicki and Karl Lendi. *Quantum dynamical semigroups and applications*, volume 717. Springer, 2007.
- [29] Goran Lindblad. On the generators of quantum dynamical semigroups. *Communications in Mathematical Physics*, 48(2):119–130, 1976.
- [30] Ravinder R Puri. *Mathematical methods of quantum optics*, volume 79. Springer Science & Business Media, 2001.
- [31] Bernhard Baumgartner, Heide Narnhofer, and Walter Thirring. Analysis of quantum semigroups with gks–lindblad generators: I. simple generators. *Journal of Physics A: Mathematical and Theoretical*, 41(6):065201, 2008.
- [32] Victor V. Albert and Liang Jiang. Symmetries and conserved quantities in lindblad master equations. *Phys. Rev. A*, 89:022118, Feb 2014. DOI: [10.1103/PhysRevA.89.022118](https://doi.org/10.1103/PhysRevA.89.022118). URL <https://link.aps.org/doi/10.1103/PhysRevA.89.022118>.
- [33] Victor V. Albert, Barry Bradlyn, Martin Fraas, and Liang Jiang. Geometry and response of lindbladians. *Phys. Rev. X*, 6:041031, Nov 2016. DOI: [10.1103/PhysRevX.6.041031](https://doi.org/10.1103/PhysRevX.6.041031). URL <https://link.aps.org/doi/10.1103/PhysRevX.6.041031>.
- [34] Daniel A Lidar, Isaac L Chuang, and K Birgitta Whaley. Decoherence-free subspaces for quantum computation. *Physical Review Letters*, 81(12):2594, 1998.
- [35] Almut Beige, Daniel Braun, Ben Tregenna, and Peter L Knight. Quantum computing using dissipation to remain in a decoherence-free subspace. *Physical review letters*, 85(8):1762, 2000.

- [36] Julio T Barreiro, Markus Müller, Philipp Schindler, Daniel Nigg, Thomas Monz, Michael Chwalla, Markus Hennrich, Christian F Roos, Peter Zoller, and Rainer Blatt. An open-system quantum simulator with trapped ions. *Nature*, 470(7335):486, 2011.
- [37] Fabio Franchini. *An introduction to integrable techniques for one-dimensional quantum systems*, volume 940. Springer, 2017.
- [38] Malte Vogl, Gernot Schaller, and Tobias Brandes. Criticality in transport through the quantum ising chain. *Phys. Rev. Lett.*, 109:240402, Dec 2012. DOI: [10.1103/PhysRevLett.109.240402](https://doi.org/10.1103/PhysRevLett.109.240402). URL <https://link.aps.org/doi/10.1103/PhysRevLett.109.240402>.
- [39] Elliott Lieb, Theodore Schultz, and Daniel Mattis. Two soluble models of an antiferromagnetic chain. *Annals of Physics*, 16(3):407–466, 1961.
- [40] S Katsura, T Horiguchi, and M Suzuki. Dynamical properties of the isotropic xy model. *Physica*, 46(1):67–86, 1970.
- [41] Mary Beth Ruskai. Beyond strong subadditivity? improved bounds on the contraction of generalized relative entropy. *Reviews in Mathematical Physics*, 6(05a):1147–1161, 1994.
- [42] Andy CY Li, F Petruccione, and Jens Koch. Perturbative approach to markovian open quantum systems. *Scientific reports*, 4:4887, 2014.
- [43] Joseph Tindall, Carlos Sanchez Munoz, Berislav Buca, and Dieter Jaksch. Quantum synchronisation enabled by dynamical symmetries and dissipation. *arXiv preprint arXiv:1907.12837*, 2019.